

# **Effect of $\text{Al}_2\text{O}_3$ / Water and Ethylene Glycol based Nanofluid on Heat Transfer Characteristics in Single Pass Multi Tube Cross Flow Heat Exchanger**

A Dissertation submitted  
In partial fulfillment of the requirements for  
the degree of

**Master of Engineering**  
in  
**Thermal Engineering**

by

**Amarinder Singh**  
**Regd. No.: 801483003**

**Under the Supervision of**

**Mr. Sumeet Sharma**  
**(Associate professor)**  
**(MED)**

**Dr. D Gangacharyulu**  
**(Professor)**  
**(CHED)**



**MECHANICAL ENGINEERING DEPARTMENT**  
**THAPAR UNIVERSITY, PATIALA**

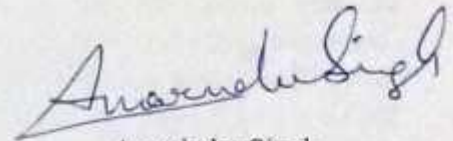
July, 2016

# CERTIFICATE

I hereby declare that the thesis entitled "Effect of  $\text{Al}_2\text{O}_3$  / Water and Ethylene Glycol based Nanofluid on Heat Transfer Characteristics in Single Pass Multi Tube Cross Flow Heat Exchanger" is an authentic record of my work carried out as requirements for the award of the degree of **Master of Engineering in Thermal Engineering** at **Thapar University, Patiala** under the supervision of **Mr. Sumeet Sharma**, Associate Professor, Mechanical Engineering Department, and, **Dr. D. Gangacharyulu**, Professor, Chemical Engineering Department, Thapar University, Patiala during July 2014 to July 2016. No part of the matter embodied in this report has been submitted to any other university or institute for the award of any degree.

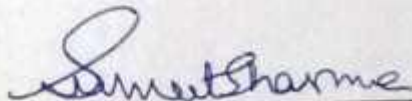
Date:

15/7/16



Amarinder Singh  
(801483003)

It is certified that the above statement made by the student is correct to the best of my/our knowledge and belief.



(Sumeet Sharma)  
Mechanical Engineering Department  
Thapar University, Patiala - 147004

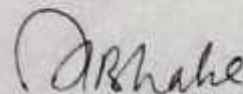


(D. Gangacharyulu)  
Chemical Engineering Department  
Thapar University, Patiala - 147004

Countersigned  
by



Dr. S.K. Mohapatra  
Head, Mechanical Engineering Department  
Thapar University, Patiala - 147004



Dean of Academic Affairs  
Thapar University, Patiala - 147004

## *Dedication*

*I dedicate this thesis to my friends Amitesh, Anuj, Himanshu, Shailabh, Gagan, Bhan aka James and Bagga who have been ever encouraging with their great patience and sarcasm, who ensured that I complete my thesis work only by the last date. I will always remember their tales and adventures which always coincided with when I used to do my thesis work and last but not the least I would like to quote my friends favourite words “ Much Appreciated.....”.*

# Acknowledgements

I would like to express my deep sense of gratitude to Mr. Sumeet Sharma, Associate Professor, Mechanical Engineering Department, Thapar University, Patiala, India & Dr. D. Gangacharyulu, Professor, Thapar University, Patiala, India for their invaluable suggestions, excellent supervision, constant encouragement, thought provoking discussions and unabashed inspiration in nurturing the work and during the preparation of manuscript throughout the research work.

I offer my special regards to Mrs. Harkirat Kaur, Research Scholars, Department of Chemical Engineering, Thapar University, Patiala, India, for providing knowledge and support in performing the experimental work throughout my research work.

I am grateful to Mr. Amit Kamboj, Laboratory Attendant, Department of Chemical Engineering, Thapar University, Patiala for providing me all the lab facilities for the successful completion of my thesis work.

Last but not least I am always grateful to my family and friends for their unconditional support, encouragement and best wishes, without which I have not come this far.

AMARINDER SINGH

# Abstract

Experimental study was conducted to determine the change in overall heat transfer coefficient and the thermo hydraulic performance characteristics of a single pass multi tube cross flow heat exchanger using  $\text{Al}_2\text{O}_3$  nanoparticles in a binary mixture of water and ethylene glycol. The base fluid was a mixture of water and ethylene glycol in 60:40% by vol. The concentration of  $\text{Al}_2\text{O}_3$  nanoparticles was 0.05% and 0.1 % by volume and the temperature was varied from 45 °C to 55 °C with flow rate from 3, 4 and 5 LPM. Thermal conductivity and viscosity were also measured. Enhancement of 6.58 % in thermal conductivity was seen at 30 °C while it was 8.23 % at 60°C. The overall heat transfer co-efficient based on the fin side heat transfer area was increased by 12.64%. The friction factor increased by 13.9% and 20.81% for 0.05% and 0.1% nanoparticle volume concentrations.

**Key words:** Nanofluids; Nanoparticles; Thermal conductivity; Viscosity ; Density ; Stability ; Heat Transfer Coefficient

# Contents

<b>Certification.....</b>	<b>I</b>
<b>Dedication.....</b>	<b>Ii</b>
<b>Acknowledgements.....</b>	<b>Iii</b>
<b>Abstract.....</b>	<b>Iv</b>
<b>Table of Contents.....</b>	<b>V</b>
<b>List of Figures.....</b>	<b>vii</b>
<b>List of Tables.....</b>	<b>Ix</b>
<b>Nomenclature .....</b>	<b>Xi</b>
<b>CHAPTER 1: Introduction .....</b>	<b>1</b>
1.1 Introduction.....	1
1.2 Preparation methods.....	2
1.2.1 Two step method.....	2
1.2.2 One step method.....	2
1.3 Stability analysis.....	3
1.4 Methods for evaluating stability.....	3
1.4.1 Sedimentation method.....	3
1.4.2 Spectral analysis method.....	3
1.4.3 Zeta potential analysis.....	3
1.4.4 Light scattering and electron microscopy techniques.....	4
1.5 Methods to increase stability.....	4
1.5.1 Use of ultrasonic agitator.....	4
1.5.2 Surface modification techniques.....	5
1.5.3 Surfactant addition.....	5
1.6 Thermo physical properties.....	6
1.6.1 Effects on viscosity.....	6
1.6.2 Effects on thermal conductivity.....	7
1.7 Heat transfer and pressure drop.....	8
1.8 Application of nanofluids.....	9
References.....	11
<b>CHAPTER 2: Literature Review.....</b>	<b>14</b>

References.....	20
<b>CHAPTER 3: Experimental setup and calibration.....</b>	<b>22</b>
3.1 Experimental setup.....	22
3.1.1 Duct.....	24
3.1.2 U tube manometer.....	25
3.1.3 Fluid reservoir.....	25
3.1.4 PID controller.....	26
3.1.5 Pump.....	27
3.1.6 Rotameter.....	27
3.1.7 RTD Pt100 temperature sensors.....	28
3.2 Ultra sonicator water bath .....	29
3.3 Thermal properties analyzer KD2 PRO .....	30
3.4 Brookfield DV-III Rheometer.....	30
<b>CHAPTER 4: Methodology and calculations.....</b>	<b>32</b>
4.1 Preparation of nanofluids.....	32
4.2 Experimental procedure.....	33
4.3 Experimental calculations.....	34
4.3.1 Air side calculations.....	34
4.3.2 Hot working fluid tube side calculations.....	35
References.....	36
<b>CHAPTER 5: Results and Discussion.....</b>	<b>37</b>
5.1 Temperature dependence of thermo-physical properties .....	37
5.1.1 Temperature dependence of density of nanofluid.....	38
5.1.2 Temperature dependence of thermal conductivity of nanofluid.....	38
5.1.3 Temperature dependence of viscosity of nanofluid.....	38
5.2 Tube side analysis of working fluid .....	39
5.2.1 Temperature dependence of Reynolds number at different flow rates	40
5.2.2 Temperature dependence of Nusselt number at different flow rates...	40
5.2.3 Temperature dependence of friction factor at different flow rates.....	41
5.2.4 Heat transfer coefficient variation with nanofluid concentration.....	42
5.2.5 Variation in pressure drop.....	43
<b>CHAPTER 6: Conclusions and Future Scope of Work.....</b>	<b>44</b>
6.1 Thermo physical Properties .....	44

6.2 Heat exchanger tube side performance .....	44
6.3 Heat exchanger overall performance.....	45
6.4 Future Scope.....	45
<b>Appendix.....</b>	<b>47</b>

## List of Figures

	<b>Page No.</b>	
Figure 3.1	Experimental Equipment	22
Figure 3.2	Layout of the Experimental Setup	23
Figure 3.3	Heat exchanger with temperature sensors	24
Figure 3.4	Duct	25
Figure 3.5	Mercury U Tube manometer	25
Figure 3.6	Reservoir tank with heating element and pump	26
Figure 3.7	PID controller	27
Figure 3.8	Pump	27
Figure 3.9	Rotameter Calibration graph	28
Figure 3.10	Temperature sensor calibration graph	29
Figure 3.11	Ultra sonicator water bath	29
Figure 3.12	KD2 Pro with KS-1 needle	30
Figure 3.13	Brookfield DV-III Rheometer	31
Figure 4.1	0.1% volume concentration Al <sub>2</sub> O <sub>3</sub> /water and ethylene glycol (60:40) nanofluid	32
Figure 4.2	Tube fin control volume	34
Figure 5.1	Effect of temperature variation on density of Al <sub>2</sub> O <sub>3</sub> /water and ethylene glycol nanofluid.	37
Figure 5.2	Dependence of Thermal Conductivity of Al <sub>2</sub> O <sub>3</sub> /water and ethylene glycol nanofluid with temperature.	38
Figure 5.3	Effects of temperature on viscosity of nanofluid.	39
Figure 5.4(a)	Reynolds number for base fluid	40
Figure 5.4(b)	Reynolds number for 0.05% Al <sub>2</sub> O <sub>3</sub>	40
Figure 5.4(c)	Reynolds number for 0.1% Al <sub>2</sub> O <sub>3</sub>	40

Figure 5.5(a)	Nusselt number for base fluid	41
Figure 5.5(b)	Nusselt number for 0.05% Al <sub>2</sub> O <sub>3</sub>	41
Figure 5.5(c)	Nusselt number for 0.1% Al <sub>2</sub> O <sub>3</sub>	41
Figure 5.6(a)	Friction factor for base fluid	42
Figure 5.6(b)	Friction factor for 0.05% Al <sub>2</sub> O <sub>3</sub>	42
Figure 5.6(c)	Friction factor for 0.1% Al <sub>2</sub> O <sub>3</sub>	42
Figure 5.7	Effects of temperature on heat transfer coefficient at different concentrations.	43
Figure 5.8	Tube side pressure drop at different concentrations	43

## List of Tables

	<b>Page No.</b>	
Table 3.1	Equipment details and specifications	23
Table 3.2	Heat exchanger specifications	24
Table 3.3	Specification single-needle (KS-1)	30
Table 3.4	Specification Brookfield DV-III Programmable Rheometer	31
Table 4.1	Properties of the Al <sub>2</sub> O <sub>3</sub> nanoparticles	32
Table A1	Rotameter calibration data	47
Table A2	Temperature sensors calibration data	47
Table A3	Conductivity of Al <sub>2</sub> O <sub>3</sub> /water and ethylene glycol nanofluid with temperature.	47
Table A4	Viscosity of nanofluid with temperature	48
Table A5	Reynolds number with temperature	48
Table A6	Nusselt number with temperature	48
Table A7	Friction factor with temperature	48
Table A8	Properties of air at 1 atm pressure	49
Table A9	Temperature data for 45°C fluid temperature at 3 LPM flowrate and air velocity of 3.3 m/s	49

## Nomenclature

$A_t$	: total heat transfer surface area, $m^2$
$A_o$	: free flow areas of the exchanger, or Cross section area of exchanger, $m^2$
$A_f$	: surface area of fin exposed to heat transfer, $m^2$
$A_{fr}$	: air side frontal area on one side of the exchanger, $m^2$
$A_{nft}$	: non fin area, $m^2$
$A_{c,t}$	: cross section area of tube, $m^2$
$A_w$	: Airways
$T_t$	: tube thickness
$T_w$	: tube width
$T_l$	: tube length for small cross section, m
$T_{t,l}$	: total tube length in core dimension, m
$T_s$	: tube sheet thickness, m
$F_t$	: fin thickness, m
$F_l$	: fin length, m
$F_w$	: fin width, m
$F_{t,l}$	: total fin length, m
$N_t$	: number of tubes one side
$N_f$	: number of fins in between two tube.
$N_s$	: total number of fins one side
$A$	: tube spacing, m
$a$	: half fin length for small cross section = (tube spacing)/2, m
$B$	: fin spacing, m
$b$	: half of tube thickness for small cross section = (fin spacing)/2, m

W	: fluid flow (air) length, m
$C_f$	: circumference of fin exposed to heat transfer, m.
$C_p$	: specific heat of fluid at constant pressure, J/kg $^{\circ}$ C.
$D_h$	: hydraulic diameter of flow passage, m
f	: friction factor, dimensionless
G	: mass velocity, kg/m <sup>2</sup> s
C	: heat capacity rate
H	: total water flow length, m
h	: heat transfer coefficient, W/m <sup>2</sup> $^{\circ}$ C
J	: Colburn factor, dimensionless
K	: fluid thermal conductivity, W/m $^{\circ}$ C
$k_f$	: thermal conductivity of fin material, W/m $^{\circ}$ C
l	: fin length for heat conduction from primary to the midpoint between plates, m
L	: non-fluid flow length, m
LPM	: Litres per minute
$f_p$	: fin parameter, m <sup>-1</sup>
P	: pressure, Pa
Pr	: Prandtl number, dimensionless
Nu	: Nusselt number
Re	: Reynolds number based on hydraulic diameter, dimensionless
$r_h$	: flow passage hydraulic radius, m
T	: fluid temperature, $^{\circ}$ C
U	: overall heat transfer coefficient, W/m <sup>2</sup> $^{\circ}$ C.
V	: volume, m <sup>3</sup> .
v	: velocity, m/s.
m	: fluid mass flow rate, kg/s.
$R_c$	: fouling resistance, W/m <sup>2</sup> $^{\circ}$ C.

$R_t$	: tube wall resistance, $W/m^2 \text{ } ^\circ C$ .
$R_h$	: fouling resistance, $W/m^2 \text{ } ^\circ C$ .
$\alpha$	: ratio of total heat transfer area of one side to its volume, $m^2/m^3$ .
$\rho$	: density, $kg/m^3$ .
$\delta$	: thickness of fin, m.
$\mu$	: fluid dynamic viscosity, Pa.s.
$\sigma$	: ratio of free flow area to frontal area, dimensionless.
$\eta_f$	: fin efficiency
$\eta_0$	: overall efficiency
$\xi$	: heat exchanger effectiveness.

### **Subscripts**

a	: air
b	: bulk
c	: cold fluid side
h	: hot fluid side
bf	: base fluid
1	: inlet condition
2	: outlet condition.

# Chapter 1

## Introduction

---

### 1.1 Introduction

Miniaturized and highly efficient thermal systems represent the current requirements of the automobile, industrial as well as residential cooling and heating systems. But the performance of the modern thermal systems is primarily limited by the lower conductivity of the fluids being used in these systems. As a result of research and technology advancements, the concept of Nanofluids was introduced. The term Nanofluids broadly refers to the fluids with particles of average size less than 100 nm dispersed in it. The presence of these particles drastically alters the thermal and transport properties of the base fluid due to which there is a wide scope of their applications. Primarily conventional fluids like water, lubricating oil and coolant additives like ethylene glycol etc. are employed as the working fluids for the heating and cooling systems. One of the major limiting factors for the low heat transfer performance of these fluids is their poor thermal conductivity. Hence the idea of dispersing solid particles in the fluid was introduced in order to improve the thermal conductivity of the fluid and thus improve their heat transferring characteristics. High conductivity of solids can be utilized in increasing the thermal conductivity of a fluid by the addition of small solid particles to the fluid. The feasibility and application of the usage of such mixtures of solid particles with sizes ranging from  $10^{-9}$  to  $10^{-7}$  meters was previously examined by many researchers.

Nanofluid is a new type of heat transfer fluid, having nanoparticles (1–100 nm) which are evenly distributed in the base fluid. These uniformly distributed nanoparticles are generally metal or metal oxides which have a great enhancing effect on the thermal conductivity of the nanofluid, thus increasing conduction and convection coefficients and allowing for higher heat transfer. Nanofluids are being examined for use as advanced heat transfer fluids for the last two decades. However, because of the complexity and variety of nanofluid systems, no particular agreement has been reached till now on the possible benefits of using these fluids for heating/cooling applications.

Nanofluid cannot be considered simple liquid-solid mixture. It is important to achieve agglomeration-free suspension for considerably long time periods without the

possibility of any changes in chemical composition of the base fluid. This can only be achieved by reducing the density difference between liquids and solids or by increased viscosity of base fluid. For two-phase systems one of the major issues is the stability of these nanofluids, and till date it has remained a challenge.

## **1.2 Preparation methods**

The preparation of nanofluids from nanoparticles can be broadly categorized under the following two methods.

### **1.2.1 Two-Step Method**

The Two-step method is the most commonly used method for preparing nanofluids. Nanoparticles, nanotubes (carbon nanotubes), nanofibers and other nanomaterials utilized in this method are produced as dry powders first by the means of chemical and physical methods. After that the powder is dispersed into a base fluid in the second step, with the help of external mixing or stirring methods like magnetic agitators, ultrasonic agitators, high-shear mixers, homogenizing or ball milling. The Two-step method is the most commonly used and economic method to prepare nanofluids in large quantities because the nanopowder manufacturing techniques have already started providing up to required industrial production levels. Because of the high surface area and surface related activity, the nanoparticles have a tendency to accumulate together. One of the important methods to improve the stability of nanoparticles in base fluids is to use surfactants which reduce surface tension of base fluids.

### **1.2.2 One-Step Method**

Because of the difficulties faced regarding stability during the mixing process in preparing nanofluids by Two-step method, the One-step method was developed. In order to reduce the accumulation of nanoparticles, Eastman et al. [2] suggested the one-step physical vapor condensation process for preparing Cu/ethylene glycol nanofluids. In this one-step method, it involves the simultaneous synthesis and dispersion of the nanoparticles in the base fluid. By this method, the drying, storage and transportation processes are removed, so the accumulation of nanoparticles is kept at a minimum. Thus the stability of fluids is greatly increased [1]. The one-step method can be used to prepare fluids with uniformly dispersed nanoparticles and these particles can be kept suspended in a stable manner. The nanoparticles so prepared have needle-like, square, polygonal or circular morphological shapes. The One step process avoids the unwanted particle aggregation quite well.

## **1.3 Stability analysis**

The sticking together of particles termed as agglomeration leads to settlement of the dispersed particles. Prolonged agglomeration can result in large deposits of particles which can further result in clogging, especially in case of micro channels where the fluid passages are already very small. Hence stability is also an important factor that needs to be considered.

## **1.4 Methods for evaluating stability**

### **1.4.1 Sedimentation method**

This method is the simplest method for evaluation of stability [3]. An external force is utilized to initiate the sedimentation. The sediment weight or the sediment volume measured after the predetermined time period represents the stability. They are said to be stable if the dispersed particle concentration remains constant with respect to time. The sedimentation method was utilized by Zhu et al. [4] during experimentation in order to establish graphite suspension stability. Most researchers capture photographs of the samples at regular time intervals for 24 hours after the nanofluid sample is prepared to determine sedimentation and hence conclude its stability [5, 6]. The only drawback of sedimentation method is the long period for observation it requires. Therefore it can be expedited by the action of a centrifugal force by placing the sample in a setup to spin it at a speed of around 3000 rpm [7]. This improved method for sedimentation is termed as Centrifugation method.

### **1.4.2 Spectral analysis method**

Spectral absorbency analysis is also an efficient method to study the stability of nanofluids. Generally the relationship between the absorbance intensity & concentration of particles in the fluid is linear. If the nanoparticles dispersed in the fluid have a characteristic absorption band in the region of 190–1100 nm wavelength, then it is a simple and reliable method to establish the stability of nanofluids. It utilizes UV-visual spectral analysis. Its advantage is that it gives quantitative results with respect to concentration of nanofluids [8].

### **1.4.3 Zeta Potential Analysis**

Zeta potential is defined as the potential difference between dispersion fluid and the layer of stationary attached to the surface of the dispersed particles. It represents the degree of

repulsion amongst similarly charged adjacent particles. The Zeta potential can be either positive or negative. Therefore suspensions with a high value of zeta potential are considered to be electrically more stable as compared to suspensions with low zeta potentials. The values of zeta potential ranging from 40-60 mV are believed to be highly stable. Kim et al. [9] performed zeta potential analysis for Au nanofluids and observed acceptable stability. Zhu et al. [10] studied Alumina-water based nanofluids at various pH levels and at different surfactant concentrations.

#### **1.4.4 Light Scattering and Electron Microscopy techniques**

Imagery analysis of the nanofluids can be done by using electron microscope namely Scanning Electron Microscope (SEM) or Transmission Electron Microscope (TEM). Usually TEM is preferred over SEM in case of nanofluids and most of researchers utilize TEM for their characterization. Cryogenic transmission electron microscope has the capability to provide a more powerful and reliable characterization technique but its available in very few laboratories. Scanning Probe Microscopy (SPM) did not find much use for characterization. A very simple method represents particle size analysis on basis of Dynamic Light Scattering (DLS). Most researchers have utilized DLS technique to determine for particle size distribution and then corroborate the results with TEM as main characterization tool. Other important characterization tools for the structure and morphology nanoparticles are the Small Angle X-ray Scattering (SAXS) and Small Angle Neutron Scattering (SANS).

### **1.5 Methods to increase stability**

#### **1.5.1 Use of ultrasonic agitators**

After nanofluids have been prepared, agglomeration may occur over time which can result in even faster sedimentation rates of particles because large clustered particles show the tendency to settle down quickly under the action of gravity alone. Ultrasonic agitation can break those clustered particles back into individual particles and it depends on how long the nanofluid sample was kept in the agitator as demonstrated by Manson et al. [11]. Wang et al. [6] Investigated two different nanofluids; carbon black-water and silver-silicon oil and they utilized high energy of cavitation for breaking clusters among particles and again it was observed that there were less clustered particles in samples that were kept in agitator for longer time durations [12].

### **1.5.2 Surface modification techniques**

This technique does not require a surfactant. It involves the addition of functional particles into the base fluids which are capable of providing very stable nanofluids. There are several examples of these modification techniques. Yang et al. [13] experimented with addition of silanes to the surface of silica nanoparticles in the solution. It was observed that there was no deposition layer formation on the heating surface after the pool boiling process. Another way to increase stability of carbon nanotubes is by adding hydroxyl groups onto their surface [14]. These techniques, although complex, have shown to increase stability of nanoparticles that otherwise tend to agglomerate. Another test was conducted to synthesize nanofluids containing single as well as double walled CNTs by wet mechanochemical reaction without the use of surfactants. Data from the infrared spectrum & zeta potential tests represented that hydroxyl groups had attached onto CNT surfaces [16].

### **1.5.3 Surfactant addition**

Surfactants added in nanofluids are also termed as dispersants. It is an easy and economical method to achieve the stability of nanofluids. Surfactants tend to have an effect on surface characteristics even when added in small quantities. They consist of a hydrophobic portion called the TAIL which is generally a long-chain hydrocarbon, and a hydrophilic portion called the HEAD. They are added to increase the surface contact of two materials which is also termed as wet ability. Generally in case of two-phase systems, the surfactant tends to position itself at the interface of the two phases and maintains a degree of continuity to some extent between the particles and the base fluid. Depending upon the type of the head, they are broadly classified into four categories namely a) nonionic (without any charge groups in its head), b) anionic (negatively charged head groups) c) cationic (with positively charged head groups) and d) amphoteric (with zwitterionic head group). Selection of the right type of surfactant is very important. Generally if the base fluid used is polar solvent then it is necessary to select water-soluble surfactants otherwise oil soluble ones can be selected. In the case of nonionic surfactants the solubility through hydrophilic/lipophilic balance (HLB) value can be evaluated. A lower HLB value indicates more oil soluble surfactants, whereas a higher HLB number represents a more water-soluble surfactant. Although it is an effective way to increase stability of nanoparticles, it can lead to several problems like contaminating heat transfer media, produce undesirable effects like foaming etc. during heating or cooling, effect thermal properties of the nanoparticles and base fluid like reduced enhancement in thermal conductivity [15].

## **1.6 Thermo physical properties**

Experimental studies have shown that the thermal conductivity of nanofluids largely depends on different factors like particle volume fraction, material used, particle size and shape, base fluid used and also the temperature. The amount and types of additives along with the acidity of the nanofluid were also responsible in the enhancement of the thermal conductivity. Dynamic thermal conductivity along with the viscosity are largely dependent on volume concentration of nanoparticle and other parameters like particle shape and its size distribution, mixtures used and slip mechanisms, dispersants, etc. Studies have also showed that thermal conductivity and viscosity both increase by adding nanoparticles in the base fluid as compared to the base fluid itself. So far till date many theoretical and experimental values have provided us with various correlations that have been proposed for thermal conductivity as well as viscosity of these fluids. However, till now no general correlations have been developed because of lack of mutual understanding on their mechanisms.

### **1.6.1 Effects on viscosity**

The particles when dispersed in a fluid may come close to each other and form aggregates of sizes greater than the original particle size which, as a result, tend to settle down due to gravity. Stability in nanofluids means that there is very low aggregation of the particles. The aggregation rate is practically determined by the collisions frequency and the probability of particles joining together during collisions. Another research was done to analyze the dispersion and stability characteristics of nanofluids prepared by dispersing CuO nanoparticles. The behavior characteristics based on concentrations by volume at high pressures of 45 MPa and viscosity at atmospheric pressure were investigated experimentally. It was observed that the effect of particle size on density was not substantial but still it could not be ignored. Also the viscosity differences were very large and required to be taken into consideration for practical applications. These viscosity differences could be explained qualitatively with the help of a theory explaining both, the state of aggregation and the distribution of particle size of the nanofluid. Tran X. Phuoc et al [17] have given some experimental observations based on the shear rate effects and particle concentrations by volume on the shear stress and the viscosity behavior of nanofluids prepared by dispersing  $\text{Fe}_2\text{O}_3$  along with Polyvinylpyrrolidone (PVP) or

Polyethylene oxide, (PEO), as a dispersant. The observations made clearly show that these fluids experienced a yield stress and behaved like shear-thinning non-Newtonian fluids. The yield stresses were reduced to Newtonian limit, as the particle volume fraction was reduced but still existed at low particle concentrations by volume.

### **1.6.2 Effects on thermal conductivity**

A large number of experimental and theoretical studies have been conducted in the literature to determine a standard correlation for thermal conductivity of nanofluids. M.M. Elias et al. [18] presented a research paper for the thermo physical properties of  $\text{Al}_2\text{O}_3$  nanoparticles dispersed into water along with ethylene glycol used as coolant in automobile radiator. The nanofluids were prepared by the two-step method utilizing an ultrasonic homogenizer but without any surfactants. Thermo physical properties like conductivity, viscosity and specific heat were determined at different volume concentrations of nanoparticles at different temperatures. The results showed that thermal conductivity, viscosity, and density of the nanofluid increased when the particle concentration was increased but the specific heat of nanofluid showed a decrease. Moreover, with increase in temperature, thermal conductivity and specific heat were increased but the viscosity and density were decreased.

Madhusree Kole, T.K. Dey [19] investigated the viscosity of the nanofluid synthesized from alumina nanoparticles dispersed in commercial car coolant. The nanofluid mixed with predetermined quantity of oleic acid surfactant was observed to be stable for more than 80 days. The effects of volume fraction and temperature on viscosity were determined. Whereas the pure base fluid exhibited Newtonian behavior at the measured temperature, it changed into a non-Newtonian fluid after the addition of a small quantity of alumina nanoparticles. Their results prove that viscosity of the nanofluid increased with increasing concentrations and decreasing temperatures. Most of the previously predicted models under estimate the values of the measured viscosity. Dependence of the nanofluid viscosity on volume fraction is predicted quite well by most of the given correlations for nanofluids that consider the effect of Brownian motion of nanoparticles. Similar results were given by other researchers also [32].

L. Syam Sundar et al. [20] investigated the experimental and theoretical effect on thermal conductivity and viscosity of magnetic  $\text{Fe}_3\text{O}_4$  water nanofluid. The nanofluid was synthesized by first preparing  $\text{Fe}_3\text{O}_4$  nanoparticles utilizing chemical precipitation method, and then a sonicator was employed to disperse them in water. Thermal conductivity &

viscosity were observed to increase with increasing particle concentration. Viscosity enhancement was more as compared to thermal conductivity enhancement at any given concentration & temperature. Theoretical correlations were predicted to give the properties of nanofluids without having to revert back to the Maxwell and Einstein correlations, respectively.

## **1.7 Heat transfer and pressure drop**

The effective enhancement of thermal conductivity is very important for the improved heat transferring behavior of the fluids. Various other variables also play important roles in the observed results. For instance, the heat transfer coefficient in the case of forced convection in tubes may be affected by several physical quantities that are related to the fluid as well as geometry of the given process system through which the flow is being tested. These quantities often are the intrinsic properties like thermal conductivity, specific heat, density or viscosity of the fluid as well as the extrinsic system properties like the tube diameter, length, flow velocity etc. A.A. Abbasian Arani et al. [22] investigated the effect of nanoparticle concentration on the convection heat transfer coefficient along with pressure drop of TiO<sub>2</sub> water nanofluids with particle concentration between 0.002 and 0.02 by volume and Reynolds ranging from 8000 to 51,000. The experimental setup used was a horizontal double tube counter-flow type heat exchanger. The results showed that by increasing the Reynolds number or particle concentration, the convective heat transfer capability increased. But it is well known that all nanofluids show higher Nusselt number as compared to the distilled water itself. But for using the nanofluid at higher Reynolds number, much more pumping power was required to compensate for the pressure drop in nanofluid, whereas the increase in the Nusselt number with respect to all Reynolds numbers is approximately the same. Hence the use of nanofluids at higher Reynolds numbers as compared to lower Reynolds numbers shows very less benefits. Deepak Kumar Agarwal et al. [23] studied the turbulent convective heat transfer characteristics of kerosene- Al<sub>2</sub>O<sub>3</sub> nanofluid in a horizontal circular experimental configuration using a closed loop setup. The purpose was to identify the possibilities of use of kerosene-Al<sub>2</sub>O<sub>3</sub> nanofluid in the regenerative cooling of the thrust chamber in a semi-cryogenic rocket engine. The particle size variation effects, effects of concentration from 0.05% to 0.5% and effects of Reynolds number on convective heat transfer & pressure drop were explained. Heat transfer performance of the nanofluid is calculated with respect to identical Reynolds number, Peclet number and velocity. Further detailed study of experimental data predicted that in most cases, heat transferring properties

were significantly higher as compared to the pure base fluid i.e. kerosene. Higher increase in heat transfer coefficient was noticed for larger sized particles compared to smaller sized ones although the measured thermal conductivity was showed to be higher for smaller sized particle. A correlation to determine the total heat transfer characteristics of nanofluids is also determined, which indicates the advantages of these fluids with respect to their thermo physical properties. The observations also highlight the importance of Prandtl number in convective heat transfer characteristics.

using computational fluid dynamics (CFD). The behavior and characteristics of pure water & pure ethylene glycol were compared with the observed results. The heat transfer coefficients from both methods were compared with those of different particles concentrations. A minute change in the friction factors was observed in the system and the convective heat transfer coefficient of the second model was quite different from that of the first model.

## **1.8 Application of nanofluids**

The concept of nanofluids came into existence about two decades ago. Their potential in heat transfer or cooling applications has continuously attracted increasing attention. Up till now, there were some research papers which presented overviews of different aspects of these nanofluids. Because of higher density chips, the design of more compact electronic components makes heat dissipation even more difficult. All advanced electrical or electronic devices are facing heat management challenges due to the increased levels of heat generation and the reduction in the surface area for heat rejection or dissipation. So a reliable heat management system is very important for the continuous and smooth working of these modern electronic devices. Generally, there are two alternatives for improving the heat dissipation for the electronic equipment. First one is to find the best geometry for cooling devices; second one is to increase their capability to transfer heat. Nanofluids with very high thermal conductivities also have high convective heat transfer coefficients when compared to their base fluids. Recent reviews showed that nanofluids can increase the heat transfer coefficient as well as the thermal conductivity of a fluid or coolant.

Nanofluids have very high potential in improving automotive industry and cooling rates of heavy-duty engine by increasing efficiency, reducing the weight and complexity of heating/cooling systems. The increased cooling rates for automobile and truck engines can also be used to reject more heat energy from higher output engines using the same sized cooling system. Also on the other hand it would be beneficial to design even more compact cooling system with radiators which are smaller and lighter. It would also be beneficial as it

would increase the performance and fuel economy and performance of cars and trucks. Nanofluids based on Ethylene glycol have recently attracted attention in the possibility of use as engine coolant [18, 24, 32] because of the low-pressure working conditions compared to a 50/50 mixture of water and ethylene glycol, which is the most commonly used automobile coolant. These nanofluids have a very high boiling point, and these can be used to increase the working temperatures of normal coolants and also remove more heat utilizing the already existing cooling systems.

In Space and Defense sectors, because of the restriction of space, weight, and available energy in space stations and aircrafts, there is a very strong demand for highly efficient heating/cooling systems which are as small in size as possible. The Nanofluids with very high heat fluxes are capable of providing the necessary cooling/heating rates in such applications and in other systems of the military or defense and space sectors, which may include military vehicles and submarines or even high-power laser. Therefore, the applications of nanofluids range widely especially in the fields where density of power is very high and the equipment needs to be smaller and lighter.

Over the last two decades, drug delivery systems based on nanoparticles have also been developed so as to increase the efficiency of the drug action. The very small-sized, customized surface improves the soluble properties and the multi functional aspects of the nanoparticles open many opportunities and create new applications in the field of biomedicines.

## References

- [1]. Y. Li, J. Zhou, S. Tung, E. Schneider, and S. Xi, “A review on development of nanofluid preparation and characterization,” *Powder Technology*, vol. 196, no. 2, pp. 89–101, 2009.
- [2]. J. A. Eastman, S. U. S. Choi, S. Li, W. Yu, and L. J. Thompson, “Anomalously increased effective thermal conductivities of ethylene glycol-based nanofluids containing copper nanoparticles,” *Applied Physics Letters*, vol. 78, no. 6, pp. 718–720, 2001.
- [3]. X. Wei and L. Wang, “Synthesis and thermal conductivity of microfluidic copper nanofluids,” *Particuology*, vol. 8, no. 3, pp. 262–271, 2010.
- [4]. H. Zhu, C. Zhang, Y. Tang, J. Wang, B. Ren, and Y. Yin, “Preparation and thermal conductivity of suspensions of graphite nanoparticles,” *Carbon*, vol. 45, no. 1, pp. 226–228, 2007.
- [5]. X. Wei, H. Zhu, T. Kong, L. Wang, “Synthesis and thermal conductivity of Cu<sub>2</sub>O nanofluids”, *Int. J. Heat Mass Transfer* 52 (19–20) (2009) 4371–4374.
- [6]. X. Q. Wang and A. S. Mujumdar, “A review on nanofluids—part I: theoretical and numerical investigations,” *Brazilian Journal of Chemical Engineering*, vol. 25, no. 4, pp. 613–630, 2008.
- [7]. Y. Hwang, J. K. Lee, C. H. Lee et al., “Stability and thermal conductivity characteristics of nanofluids,” *Thermochimica Acta*, vol. 455, no. 1-2, pp. 70–74, 2007.
- [8]. X. Yang and Z. H. Liu, “A kind of nanofluid consisting of surface-functionalized nanoparticles,” *Nanoscale Research Letters*, vol. 5, no. 8, pp. 1324–1328, 2010.
- [9]. S. P. Jang and S. U. S. Choi, “Cooling performance of a microchannel heat sink with nanofluids,” *Applied Thermal Engineering*, vol. 26, no. 17-18, pp. 2457–2463, 2006.
- [10]. H. Xie, W. Yu, and Y. Li, “Thermal performance enhancement in nanofluids containing diamond nanoparticles,” *Journal of Physics D*, vol. 42, no. 9, Article ID 095413, 2009.
- [11]. P. Sharma, S Sharma, D. Gangacharyulu, “Review on thermal properties of nanofluids and factors affecting the same”, *International Journal of Engineering Science and Technology*, Vol. 6 No.8, pp. 0975-5462, 2014.
- [12]. S. Kumar, S Sharma, D. Gangacharyulu, “Coding and evaluation and optimum selection of nanofluid in plate heat exchanger”, *International Journal of Engineering Science and Technology*, vol. 6, no. 8, 2014.

- [13]. M. Kole and T. K. Dey, "Thermal conductivity and viscosity of Al<sub>2</sub>O<sub>3</sub> nanofluid based on car engine coolant," *Journal of Physics D*, vol. 43, no. 31, Article ID 315501, 2010.
- [14]. Y. T. Chen, W. C. Wei, S. W. Kang, and C. S. Yu, "Effect of nanofluid on flat heat pipe thermal performance," in *Proceedings of the 24th IEEE Semiconductor Thermal Measurement and Management Symposium (SEMI-THERM '08)*, March 2006.
- [15]. H. Xie and L. Chen, "Adjustable thermal conductivity in carbon nanotube nanofluids," *Physics Letters Section A*, vol. 373, no. 21, pp. 1861–1864, 2009.
- [16]. M. Kole and T. K. Dey, "Thermal conductivity and viscosity of Al<sub>2</sub>O<sub>3</sub> nanofluid based on car engine coolant," *Journal of Physics D*, vol. 43, no. 31, Article ID 315501, 2010.
- [17]. D. P. Kulkarni, D. K. Das, and R. S. Vajjha, "Application of nanofluids in heating buildings and reducing pollution," *Applied Energy*, vol. 86, no. 12, pp. 2566–2573, 2009.
- [18]. L. Chen and H. Xie, "Surfactant-free nanofluids containing double- and single-walled carbon nanotubes functionalized by a wet-mechanochemical reaction," *Thermochimica Acta*, vol. 497, no. 1-2, pp. 67–71, 2010.
- [19]. V. Trisaksri and S. Wongwises, "Critical review of heat transfer characteristics of nanofluids," *Renewable and Sustainable Energy Reviews*, vol. 11, no. 3, pp. 512–523, 2007.
- [20]. X. Q. Wang and A. S. Mujumdar, "Heat transfer characteristics of nanofluids: a review," *International Journal of Thermal Sciences*, vol. 46, no. 1, pp. 1–19, 2007.
- [21]. X. Q. Wang and A. S. Mujumdar, "A review on nanofluids—part I: theoretical and numerical investigations," *Brazilian Journal of Chemical Engineering*, vol. 25, no. 4, pp. 613–630, 2008.
- [22]. H. T. Zhu, Y. S. Lin, and Y. S. Yin, "A novel one-step chemical method for preparation of copper nanofluids," *Journal of Colloid and Interface Science*, vol. 277, no. 1, pp. 100–103, 2004.
- [23]. Y. Li, J. Zhou, S. Tung, E. Schneider, and S. Xi, "A review on development of nanofluid preparation and characterization," *Powder Technology*, vol. 196, no. 2, pp. 89–101, 2009.
- [24]. W. Yu, H. Xie, X. Wang, and X. Wang, "Highly efficient method for preparing homogeneous and stable colloids containing graphene oxide," *Nanoscale Research Letters*, vol. 6, p. 47, 2011.

- [25]. H. T. Zhu, C. Y. Zhang, Y. M. Tang, and J. X. Wang, "Novel synthesis and thermal conductivity of CuO nanofluid," *Journal of Physical Chemistry C*, vol. 111, no. 4, pp. 1646–1650, 2007.
- [26]. H. J. Kim, I. C. Bang, and J. Onoe, "Characteristic stability of bare Au-water nanofluids fabricated by pulsed laser ablation in liquids," *Optics and Lasers in Engineering*, vol. 47, no. 5, pp. 532–538, 2009.
- [27]. X. J. Wang, X. Li, and S. Yang, "Influence of pH and SDBS on the stability and thermal conductivity of nanofluids," *Energy and Fuels*, vol. 23, no. 5, pp. 2684–2689, 2009.
- [28]. D. Zhu, X. Li, N. Wang, X. Wang, J. Gao, and H. Li, "Dispersion behavior and thermal conductivity characteristics of Al<sub>2</sub>O<sub>3</sub>-H<sub>2</sub>O nanofluids," *Current Applied Physics*, vol. 9, no. 1, pp. 131–139, 2009.
- [29]. L. Chen and H. Xie, "Properties of carbon nanotube nanofluids stabilized by cationic gemini surfactant," *Thermochimica Acta*, vol. 506, no. 1-2, pp. 62–66, 2010.
- [30]. L. Wang and J. Fan, "Nanofluids research: key issues," *Nanoscale Research Letters*, vol. 5, no. 8, pp. 1241–1252, 2010.
- [31]. J. Albadr, S. Tayal, M Talasadi, "Heat transfer through heat exchanger using Al<sub>2</sub>O<sub>3</sub> nanofluid at different concentrations", *Case studies in thermal engineering*, vol. 1, no. 1, pp. 38-44, 2013.
- [32]. D. Tiwari, A. Paul, "Experimental study on heat transfer enhancement by using water alumina nanofluid ina heat exchanger", *International Journal of Advance Research In Science And Engineering*, Vol.4, no. 05, pp. 192-200, 2015.

# Chapter 2

## LITERATURE REVIEW

---

**Ali et al. [1]** studied the effect of Alumina/water nanofluids on the thermal performance of cooling system of an automobile radiator.  $\text{Al}_2\text{O}_3$ /water nanofluids were prepared at five different concentrations viz. 0.1, 0.5, 1, 1.5 and 2 % by volume. Gradual enhancement in heat transfer was observed with particle volume concentration of 0.1, 0.5 and 1.0 % and was optimum at 1.0 % while it declined with further increment in particle volume concentration. The maximum percentage increase of the heat transfer rate, heat transfer coefficient, and Nusselt number of nanofluid was found 14.79, 14.72, and 9.51, respectively, which take place at maximum load of 1 KW and at particle volume concentration of 0.01.

**Jalal et al. [2]** conducted the experiments to study the effect of CuO/water nanofluids on convective heat transfer performance of a heat sink. Four different nanoparticle volume concentrations i.e. 3.5, 4, 4.5 and 5 % were used. Experimental results verified that the overall heat transfer coefficient improved and thermal resistance of the heat sink declined. They concluded that increasing the particle volume concentration results in an increment in the heat transfer coefficient.

**Mohammed et al. [3]** reviewed the effect of nanofluids on the heat transfer characteristics of micro channel heat exchanger. They reported that heat transfer rate can be increased significantly at the cost of increased friction factor. They recommended to understand the heat transfer phenomenon related to nanofluids more deliberately and proper study of nanofluid preparation techniques.

**Garg et al. [4]** investigated the thermal conductivity and viscosity of ethylene glycol based copper nanofluids. By using water as solvent, they prepared copper nanofluid with the help of chemical reaction method and then dispersed it into ethylene glycol by using sonication. They prepared nanofluid without adding any surfactant. Particle volume concentration was varied from 0.4 to 2%. Transient hot wire method was used to measure thermal conductivity of nanofluids of different concentrations. They concluded that because of higher increment in viscosity as compared to thermal conductivity, the nanofluids are not suitable in the existing thermal system. However, the advantages of increased thermal

conductivity could be beneficial by increasing the tube diameter in the application where the size of thermal equipments is of lesser importance.

**Bozorgan et al. [5]** studied the effect of Al<sub>2</sub>O<sub>3</sub>/water nanofluids on the performance of an automotive diesel engine cooling system. Nanofluids were prepared by using  $\gamma$ -Al<sub>2</sub>O<sub>3</sub> nanoparticles of 20 nm mean size and dispersing them in water. The nanofluids were used as coolant in automotive diesel engine radiator. Overall heat transfer enhancement was investigated at different particle volume concentrations in turbulent flow region. Results showed that while keeping the particle volume concentration as constant, the pumping power was decreased with the vehicle speed. Concentration of particles increased the viscosity and density of nanofluids which consequently increased the friction factor.

**Sheikhzadeh et al. [6]** analyzed the thermal performance of a car radiator while using copper/ethylene glycol as coolant. It was found that the overall heat transfer coefficient of air side was increased considerably by increasing Reynolds number and particle volume fraction of nanofluids, consequently the heat transfer rate was increased. They observed that when particle volume concentration increased from 0 to 5 %, overall heat transfer coefficient and heat transfer rate were increased by 64.3 % and 26.9 %, respectively. They also found that when Reynolds number increased from 4000 to 6000, overall heat transfer coefficient of air and nanofluid were increased by 4.5 % and 12.4 %, respectively. They concluded that heat transfer performance of radiator was better in hot weather of 50°C as compared to weather of 20°C.

**Leong et al. [7]** investigated the performance of an automotive car radiator by using Cu/EG nanofluids as coolant. Results were compared by taking Reynolds number of air and coolant as 6000 and 5000, respectively. They found that heat transfer rate was increased by 3.8 % by adding 2 % of Cu nanoparticles. Thermal performance of heat exchanger was found highly dependent on air and coolant Reynolds number. An increment of 42.7 % and 45.2 % was observed when air's Reynolds number was increased from 4000 to 6000 for ethylene glycol and Cu/EG nanofluid, respectively. While, thermal performance was increased by only 0.9 % and 0.4 % when coolant Reynolds number was increased from 5000 to 7000 for ethylene glycol and Cu/EG nanofluid, respectively. They observed that frontal area of heat exchanger was reduced by 18.7 % by adding 2% of Cu nanoparticles into the base fluid. Pumping power for nanofluid was found 12.13 % higher than that with pure ethylene glycol, while keeping volumetric flow rate of nanofluid constant to 0.2 m<sup>3</sup>/s.

**Heris et al. [8]** investigated the heat transfer characteristics of a circular tube while using Al<sub>2</sub>O<sub>3</sub>/water nanofluids as heat transfer fluid. Experiments were carried out at constant wall temperature boundary condition and in laminar flow region. Variation of Nusselt number with Reynolds number and Peclet number was investigated. Results showed that heat transfer coefficient increases with particle volume concentration and Peclet number. They concluded that along with increased thermal conductivity, Brownian motion of particles, chaotic movement and dispersion of particles plays a vital role in the heat transfer enhancement.

**Nieh et al. [9]** employed Al<sub>2</sub>O<sub>3</sub>/water and TiO<sub>2</sub>/water nanofluids in air cooled radiator to improve the performance. Thermo-physical properties of nanofluids were measured at different nanoparticle volume concentration and then pressure drop and heat dissipation rate were measured at different Reynolds number. Efficiency factor and heat dissipation rate was greater for nanofluids as compared to that with ethylene glycol/water solution. They concluded that the TiO<sub>2</sub>/water nanofluids showed the greater enhancement than Al<sub>2</sub>O<sub>3</sub>/water nanofluids. Heat dissipation rate was enhanced by 25.6% , 6.1% improvement for pressure drop was seen , pumping power was increased by 2.5 % and efficiency factor has 27.2% enhancement as compared to ethylene glycol/water mixture.

**Elias et al. [10]** experimentally investigated the thermo-hydraulic performance of car coolant system using nanofluids as coolant. Nanofluids were prepared using Al<sub>2</sub>O<sub>3</sub> nanoparticles and base fluid as a mixture of water and ethylene glycol. Two step method was used to prepare nanofluids. Various thermo-physical properties of nanofluids such as density, viscosity, thermal conductivity and specific heat were measured at different temperatures ranging from 10°C to 50°C. Different volume concentrations of nanoparticles were used varying from 0 to 1 %. Results showed that density, viscosity and thermal conductivity were enhanced with particle volume concentration while specific heat of nanofluids was decreased. With increasing temperature, thermal conductivity and specific heat were increased while density and viscosity were decreased. Enhancement in average thermal conductivity was observed 3.26 % and 8.30 % with temperature and particle volume concentration, respectively.

**Hwa-Ming Nieh et al. [11]** Used Al<sub>2</sub>O<sub>3</sub> and TiO<sub>2</sub> nanoparticles in air cooled radiator to enhance the performance. Viscosity, thermal conductivity and specific heat of nanocoolant was measured at different nanoparticle concentration and then pressure drop, heat dissipation capacity, pumping power was evaluated at different flow rates. Results showed

the relationship between pumping power and heat dissipation capacity with the help of efficiency factor. Efficiency factor and heat dissipation is higher for nanocoolant than Ethylene glycol/water mixture.  $\text{TiO}_2$  showed the greater enhancement than  $\text{Al}_2\text{O}_3$ . Maximum enhancement ratio was 25.6% for heat dissipation rate, 6.1% enhancement for pressure drop, 2.5% enhancement for pumping power and efficiency factor has 27.2% enhancement as compared to Ethylene glycol/water mixture.

**Sandesh S. Chougale et al. [12]** done experiment on car radiator by using carbon nanotubes (CNT) and  $\text{Al}_2\text{O}_3$  nanoparticles in water with four different concentration range from (0.15 to 1 vol.%). Flow rate was varied between 2l/min to 5 l/min. Forced convective heat transfer performance was studied and results showed that at 1% vol. nanoparticle maximum heat transfer enhancement was 90.76% and 52.03% for CNT and  $\text{Al}_2\text{O}_3$  nanofluid respectively was achieved. As the coolant mass flow rate increased heat transfer performance was increased for both the nanocoolant. CNT nanofluid showed massive enhancement as compared  $\text{Al}_2\text{O}_3$  nanofluid because CNT had high aspect ratio, high thermal conductivity, and low thermal resistance. As the concentration of nanoparticle was increased thermal conductivity was also increased hence cooling performance was also increased.

**Naraki M et al. [13]** took  $\text{CuO}$ /water nanofluids in car radiator under laminar condition ( $100 \leq \text{Re} \leq 1000$ ) at 0.4 % concentration by volume and about 8% enhancement is achieved over distilled water. Due to increase in thermal conductivity and Brownian motion of nanoparticles enhancement was increased. Flow rate increment in nanofluids lead to increase in overall heat transfer coefficient but as inlet temperature of nanofluid increased from  $50^\circ\text{C}$  to  $80^\circ\text{C}$  overall heat transfer coefficient decreased. There were three factors for that decrement a) as the temperature increased viscosity of nanofluid decreased much greater than density which leads to higher Reynolds number. b) At low viscosity of nanofluids the particles alignment was very rapid leading to less contact between nanoparticles. c) Thermal conductivity become lower as the particles depleted near the wall surface. For air side Reynolds number as it increased the overall heat transfer coefficient increased.

**Navid Bozorgan et al. [14]**  $\gamma\text{-Al}_2\text{O}_3$  with 20 nm mean sized nanoparticles were used in water as coolant in automotive diesel engine radiator. Turbulent conditions were taken for overall heat transfer enhancement at different volume fractions. Results showed that at same concentration the pumping power decreased as the speed of vehicle increased,

and at different concentrations the power increased as the concentration increased at same speed. Concentration increased the viscosity and density of nanofluid increased as a result pressure drop increased which lead to increment in friction factor.

**Leong et al. [15]** investigated the performance of heat transfer coefficient of car radiator with water and ethylene glycol as coolant. There was 3.8% enhancement in heat transfer coefficient with 2% concentration of copper nanoparticle in water when air Reynolds number is 6000 and for coolant it was 5000. When ethylene glycol was used as coolant with 2% concentration of copper nanoparticles only 0.9% enhancement was occurred at 4000 and 6000 Reynolds number for ethylene glycol and air respectively. 0.4% of enhancement was achieved when only ethylene glycol used as coolant. Power was increased by 12.13 % and reduction in frontal area was 18.7%.

**Das et al. [16]** investigated the thermal conductivity enhancement with temperature of  $\text{Al}_2\text{O}_3$  CuO water-based nanofluids. Temperature Oscillation technique was used to measure the thermal conductivity. Average diameter of alumina particles was 38.4 nm and for CuO was 28.6 nm the experimental results showed that with increased in temperature thermal conductivity increased. Nanofluid containing smaller particles (CuO) showed greater enhancement in thermal conductivity with temperature. Enhancement in conductivity also depended on particle concentration, as concentration increased thermal conductivity increased.

**Arani et al. [17]** investigated that the convective heat transfer coefficient and pressure drop was affected by particle concentration.  $\text{TiO}_2$  (30 nm) nanoparticle in deionised water is used, Reynolds number was between 8,000-51,000. As the Reynolds number was increased the Nusselt number also increased, but higher value of Reynolds number leads to high power consumption to compensate the pressure drop. Based on his experimental results they concluded that, for a given Reynolds number Nusselt number increased as the concentration of nanofluid increased. Thermal performance of all Reynolds number is examined by using high concentration of nanofluid having high Nusselt number.

**Murshed et al. [18]** studied the thermal conductivity enhancement of  $\text{TiO}_2$  and  $\text{Al}_2\text{O}_3$  nanoparticles with water as base fluid affected by surfactant and nanoparticle cluster formation in base fluid. This happened commonly when two step process for preparation of nanofluid and these nanoparticle agglomerates settled down in container. Cluster formation is studied by using transmission electron microscope (TEM). He observed that as the concentration of nanoparticles is increased the agglomerate or cluster

formation between nanoparticles is increased. This cluster formation reduced the thermal conductivity enhancement. Agglomerate formation depended on particle size, shape, concentration, viscosity of base fluid. Large size of cluster formation at high concentration leads to free region in base fluid and provide high thermal resistance which reduce the enhancement in conductivity. Remedy for nanofluid clustering is sonication and surfactants. They break down the large agglomerate and offer stability in nanoparticles and enhance the thermal conductivity. Cetyl trimethyl ammonium bromide (CTAB) surfactant is used in small amount to make nanoparticles stable and improve the dispersion behavior of nanoparticle, Adsorption of surfactant in fluid leads to electrostatic repulsive force and hydrophobic surface forces.

**Xuan et al. [19]** studied the effect of Cu nanoparticles concentration (with different volume fraction) on heat transfer enhancement. Coefficient of convective heat transfer increased with increased in flow velocity and volume fraction of nanoparticle for Reynolds number between 10,000-25,000. It may be noted that the heat transfer coefficient was larger than that of base fluid alone at same flow velocity. At high concentration viscosity of nanofluid increased and holds back the heat transfer enhancement because as viscosity was increased turbulence in flow decreased. Energy transfer rate increased by random motion between the particles in suspension.

**Jahar sarkar et al. [20]** used 20% ethylene glycol and 80% water to form ethylene glycol/water mixture (EG/water). Four type of nanoparticles are used Cu, SiC, Al<sub>2</sub>O<sub>3</sub>, and TiO<sub>2</sub> to see the effect of these particle in coolant for improvement in cooling capacity, effectiveness and reduction in pumping power. Results showed that SiC yield best result in performance in radiator followed by Al<sub>2</sub>O<sub>3</sub>, TiO<sub>2</sub> and Cu respectively. Maximum 15.34% enhancement in cooling capacity for SiC, 14.33% for Al<sub>2</sub>O<sub>3</sub>, 14.03% for TiO<sub>2</sub>, 10.20% for Cu. Cooling capacity was increased as the mass flow rate of air was increased. This was happened because heat transfer coefficient increased and effectiveness was decreased. Results showed that Cu based nanofluid had least cooling capacity and effectiveness when compare to other. As mass flow rate of coolant increased cooling capacity and effectiveness was increased. Cu required less power for pump as compared to other when inlet temperature of nanofluid was increased. Heat transfer rate was increased but there was very small increment in effectiveness. For each nanofluid second law efficiency and effectiveness was improved.

## References

- [1]. Ali, M., El-Leathy, A. M., & Al-Sofyany, Z. (2014). "The Effect of Nanofluid Concentration on the Cooling System of Vehicles Radiator". *Advances in Mechanical Engineering*, 6, 962510.
- [2]. Jalal, M., Meisami, H., & Pouyagohar, M. (2013). "Experimental Study of CuO/Water Nanofluid Effect on Convective Heat Transfer of a Heat Sink." *Middle-East Journal of Scientific Research*, 13(5), 606-611.
- [3]. Mohammed, H. A., Bhaskaran, G., Shuaib, N. H., & Saidur, R. (2011). "Heat transfer and fluid flow characteristics in microchannels heat exchanger using nanofluids: a review." *Renewable and Sustainable Energy Reviews*, 15(3), 1502-1512.
- [4]. Garg, J., Poudel, B., Chiesa, M., Gordon, J. B., Ma, J. J., Wang, J. B., ... & Chen, G. (2008). "Enhanced thermal conductivity and viscosity of copper nanoparticles in ethylene glycol nanofluid." *Journal of Applied Physics*, 103(7), 074301.
- [5]. Bozorgan N., Krishnakumar K. & Bozorgan N. (2013). "The Performance Evaluation of Overall Heat Transfer and Pumping Power of  $\gamma$ -Al<sub>2</sub>O<sub>3</sub>/water Nanofluid as Coolant in Automotive Diesel Engine Radiator". *ANUL XX*, NR. 1, ISSN 1453 – 7397.
- [6]. Ghanbarali S., Mohammadhadi H. & Hamed J. (2014). "Analysis of Thermal Performance of a Car Radiator Employing Nanofluid." *International Journal of Mechanical Engineering and Applications*. 2(4), 47-51.
- [7]. Leong, K. Y., Saidur, R., Kazi, S. N., & Mamun, A. H. (2010). "Performance investigation of an automotive car radiator operated with nanofluid-based coolants (nanofluid as a coolant in a radiator)". *Applied Thermal Engineering*, 30(17), 2685-2692.
- [8]. Heris, S. Z., Esfahany, M. N., & Etemad, S. G. (2007). "Experimental investigation of convective heat transfer of Al<sub>2</sub>O<sub>3</sub>/water nanofluid in circular tube". *International Journal of Heat and Fluid Flow*, 28(2), 203-210.
- [9]. Nieh, H. M., Teng, T. P., & Yu, C. C. (2014). "Enhanced heat dissipation of a radiator using oxide nano-coolant". *International Journal of Thermal Sciences*, 77, 252-261.
- [10]. Elias, M. M., Mahbubul, I. M., Saidur, R., Sohel, M. R., Shahrul, I. M., Khaleduzzaman, S. S. & Sadeghipor, S. (2014). "Experimental investigation on the thermo-physical properties of Al<sub>2</sub>O<sub>3</sub> nanoparticles suspended in car radiator coolant". *International Communications in Heat and Mass Transfer*, 54, 48-53

- [11]. Nieh Hwa-Ming, Teng Tun-Ping, Yu Chao-Chieh, (2014) , “Enhanced heat dissipation of a radiator using oxide nano-coolant”, *International Journal of Thermal Sciences* Vol. 77, 252-261.
- [12]. Chougule Sandesh S., Sahu S. K., (2014), “Comparative Study of Cooling Performance of Automobile Radiator Using Al<sub>2</sub>O<sub>3</sub>-Water and Carbon Nanotube-Water Nanofluid”, *Journal of Nanotechnology in Engineering and Medicine* Vol. 5, 011001-1.
- [13]. Naraki M, Peyghambarzadeh S.M, Hashemabadi S.H, Vermahmoudi Y, (2013), “Parametric study of overall heat transfer coefficient of CuO/water nanofluids in a car radiator”, *International Journal of Thermal Sciences* Vol. 66, 82-90.
- [14]. Bozorgan Navid, Krishnakumar Komalangan, Bozorgan Nariman, (2013), “The Performance Evaluation of Overall Heat Transfer and Pumping Power of  $\gamma$  - Al<sub>2</sub>O<sub>3</sub>/water Nanofluid as Coolant in Automotive Diesel Engine Radiator”, *ANUL XX*, NR. 1, ISSN 1453–7397.
- [15]. Leong K.Y., Saidur R., Kazi S.N., Mamun A.H., (2010), “ Performance investigation of an automotive car radiator operated with nanofluid based coolants (nanofluid as a coolant in a radiator)”, *Applied Thermal Engineering* Vol. 30, 2685-2692.
- [16]. S.K.Das, N. Putra, P. Thiesen and W. Roetzel., "Temperature dependence of thermal conductivity enhancement for nanofluids", -*transactions of ASME. Journal of Heat Transfer* Vol 125, 567-574.
- [17]. Arani Abbasian A.A, Amani J, (2012), "Experimental study on the effect of TiO<sub>2</sub>-water nanofluid on heat transfer and pressure drop" , *Experimental Thermal and Fluid Science* Vol. 42, 107-115.
- [18]. S. M. Sohel Murshed, C. A. Nieto de Castro, and M. 1. V. Lourenco, (2012), "Effect of Surfactant and Nanoparticle Clustering on Thermal Conductivity of Aqueous Nanofluids" *Journal of Nanofluids* Vol. 1, 175-179.
- [19]. Xuan Yimin, Li Qiang, (2003), "Investigation on Convective Heat Transfer and Flow Features of Nanofluids", *Journal of Heat Transfer*, Vol. 125, 151-155.
- [20]. Sarkar Jahar, Tarodiya Rahul , (2013), “Performance analysis of louvered fin tube automotive radiator using nanofluids as coolants”, *Int. J. Nanomanufacturing*, Vol. 9, No. 1.

# Chapter 3

## Experimental Setup and Calibration

---

### 3.1 Experimental Setup

Several research papers have suggested that the nanofluids improved the performance of heat exchangers because of their higher thermal conductivities as compared to conventional heat transfer fluids like oil, ethylene glycol, water etc. For this experimental study  $\text{Al}_2\text{O}_3$  nanoparticles dispersed in a binary mixture of water and ethylene glycol in 60:40% by vol. were utilized to study effects on a single pass multiple tube cross flow heat exchanger. The experimental setup is arranged as shown in the figure 3.1.



**Figure 3.1:** Experimental Equipment: (1) Display, (2) Air flow duct, (3) Forced draft fan, (4) PID controller, (5) Rotameter, (6) By pass valve, (7) Reservoir tank, (8) U tube manometer, (9) Heat exchanger.

As shown the setup consists of a cross flow heat exchanger fixed at the end of the duct through which air is supplied by a forced draft fan with speed regulator at the other end of the duct. Temperature sensors are positioned at different points on the heat exchanger and connected to a temperature display. A U-tube manometer, flow lines, two centrifugal pumps, bypass valve, reservoir with heating element and a PID controller complete the fluid flow circuit. Performance was evaluated at three different hot fluid inlet temperatures i.e. 45 °C, 50

°C and 55 °C at three different flow rates of 180, 240 and 300 LPH. Velocity of cold air by forced draft fan was varied at 3.4 m/s, 5.8 m/s and 6.4 m/s. First the experiment was carried out using distilled water as working medium, then mixture of water and ethylene glycol in 60:40% by vol. and then Al<sub>2</sub>O<sub>3</sub> nanofluids of 0.2% and 0.4% by wt. concentration were added to above solution to conduct the experiment.

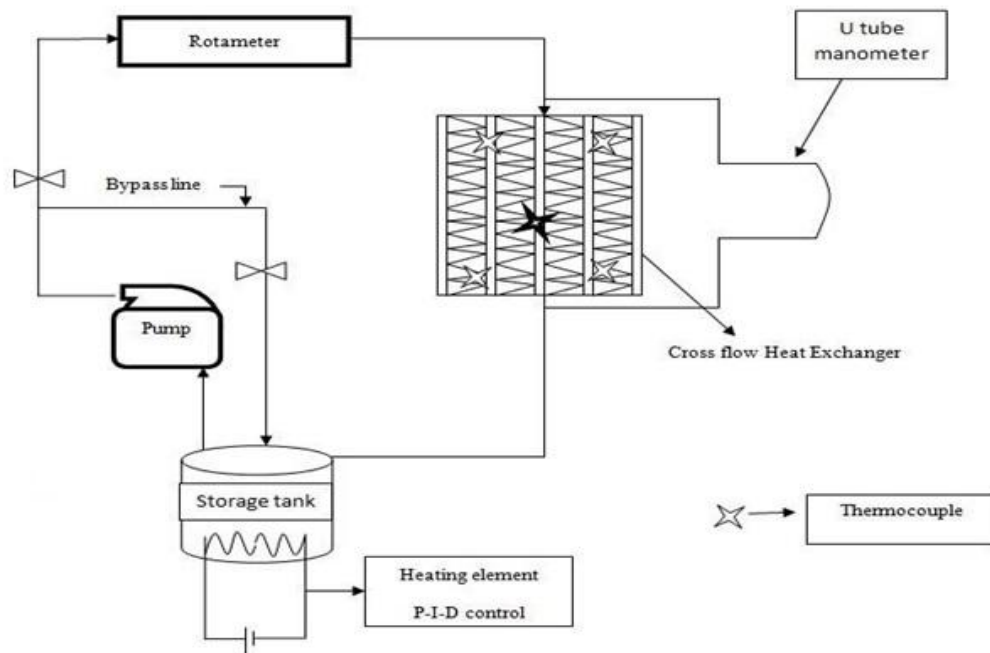


**Figure 3.2:** Layout of the Experimental Setup

**Table 3.1:** Equipment details and specifications

S.No.	Product	Specification
1	Cross flow heat exchanger	Single pass multi tube cross flow compact heat exchanger with flat tubes having semicircular ends.
2	Duct	Made of GI sheet 18 gauge.
3	U-tube manometer	Pressure drop across radiator.
4	Rotameter	Capacity 0-540 LPH.
5	Temperature sensor	RTD PT-100 type.
6	Water tank	Stainless steel
7	Heating element	3000W power.
8	PID controller	Selec TC 303
9	Anemometer	AM 804 CFM/CMM



**Figure 3.3:** Heat exchanger with temperature sensors

**Table 3.2:** Heat exchanger specifications

Cross flow core dimensions	Height	154 mm
	Width	194 mm
	Thickness	21 mm
Fin per inches	FPI	56

Heat Exchanger Areas	Tube	0.255 m <sup>2</sup>
	Fin Area	1.106 m <sup>2</sup>
	Total	1.361 m <sup>2</sup>
Front Face Area	Total	0.030 m <sup>2</sup>

Fin Length	21 mm
Fin Width	3.5 mm
Fin Thickness	0.1 mm
Fin Type	Multi Louver

Tubes Rows	No.	2
Tubes	Total	38
Tube Thickness		0.4 mm
Tube Space		5.0 mm

### 3.1.1 Duct

For a uniform flow of air over the heat exchanger, a duct of rectangular cross section made of galvanized iron sheets of 15 gauge thickness was used. The first 0.25 m length of duct was formed as a converging section followed by a uniform rectangular cross section to 1.25 m length. A forced draft fan was installed at the convergent section. Heat exchanger was fixed on the end of uniform section. Another honey comb structure was fixed at the

converging section end to obtain uniform flow of air through the duct. The forced draft fan was regulated to vary the flow rate of air passing over the heat exchanger.



**Figure 3.4:** Duct

### 3.1.2 U tube manometer

A Differential mercury U tube manometer was setup to measure the pressure drop between inlet and outlet for the working fluid. The differential U-tube manometer is shown below is indicative of energy consumed for pumping.



**Figure 3.5:** Mercury U Tube manometer

### 3.1.3 Fluid Reservoir

The fluid reservoir made of stainless steel was setup with a heating element to heat the working fluid. The capacity was 5.5 liters. Pump was setup in reservoir to pump the hot fluid whose temperature was controlled. A heating element of 3000W power was installed to heat

the working fluid. The heating element power supply was regulated by the PID controller. Figure 3.6 shows reservoir tank.



**Figure 3.6:** Reservoir tank with heating element and pump

### **3.1.4 PID controller**

A Proportional-Integral-Derivative (PID) control was used as it is the most commonly used control algorithm used in the industry. The PID algorithm employs three basic coefficients integral, proportional and derivative. The proportional component depends only on the difference between the set point and the process variable and is called the Error term. The proportional gain ( $K_c$ ) determined the ratio of output response to the error signal. The integral component estimates the error term over time. This results in even a small error term to cause the integral component to increase slowly. The integral response continuously increases over time till the error becomes zero, so the final effect is to drive the Steady-State error to zero. The derivative component results in the output to decrease if the process variable is increasing quickly. The derivative response is directly proportional to the rate of change of the process variable. Increasing the derivative time ( $T_d$ ) parameter results in the control system to strongly react to the changes in the error term and increases the speed of the overall response of the control system. Figure 3.7 shows the PID controller.



**Figure 3.7:** PID controller

### **3.1.5 Pump**

Two pumps were used one to circulate the working fluid and another was used to agitate the fluid in tank itself so that nanoparticles remained suspended in base fluid. The Second pump also acted as an agitator which avoided evaporation and local heating of fluid close to the surface of heating element.



**Figure 3.8:** Pump

### **3.1.6 Rotameter**

A Rotameter was installed to measure flow rate of working fluid. For the calibration of rotameter, flow rates were calculated with the help of a stopwatch and a measuring beaker. The calibration graph is as follows.

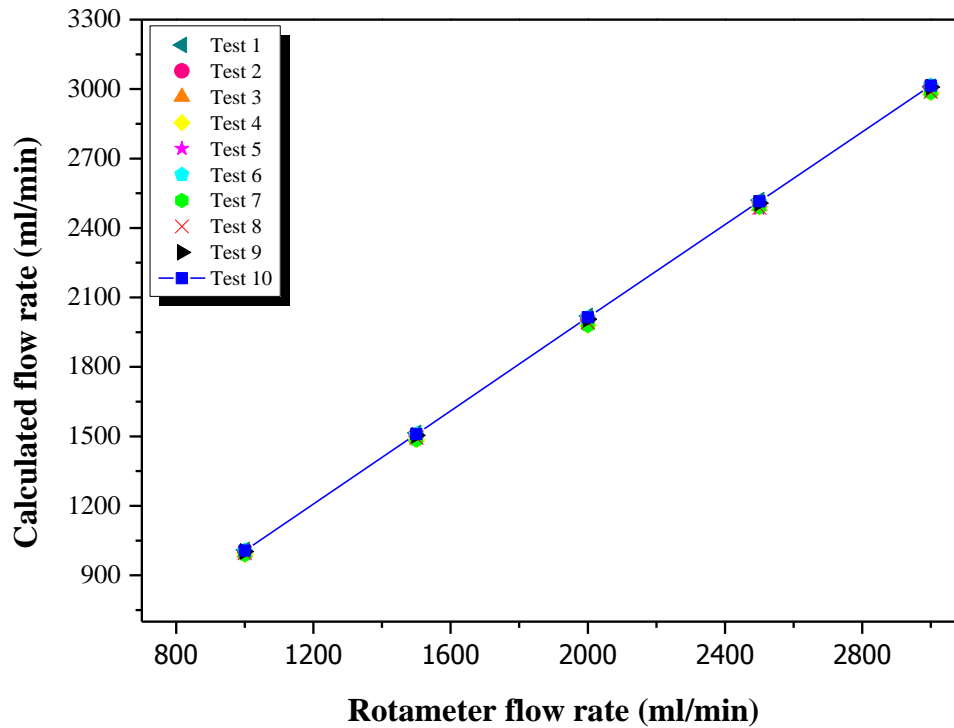


**Figure 3.9:** Rotameter Calibration graph

### 3.1.7 RTD Pt 100 temperature sensors

RTD is the abbreviation for resistance temperature detector as shown in Fig. Resistance of conductor varies linearly with temperature. Due to its high resistivity, least amount of material is used for the RTD. Pt is for platinum and 100 signifies its resistance value at 0°C temperature. Platinum can withstand very high temperatures and is therefore the most commonly used. It provides high accuracy over a wide range of temperature (-200 to +850 °C). Total nine temperature sensors were used on cross flow heat exchanger to get the air side as water side temperature readings. Four were inserted in heat exchanger to measure the hot fluid temperature at inlet as well as outlet. Four were fixed at the front side also called air outlet and one on back side also called inlet of heat exchanger.

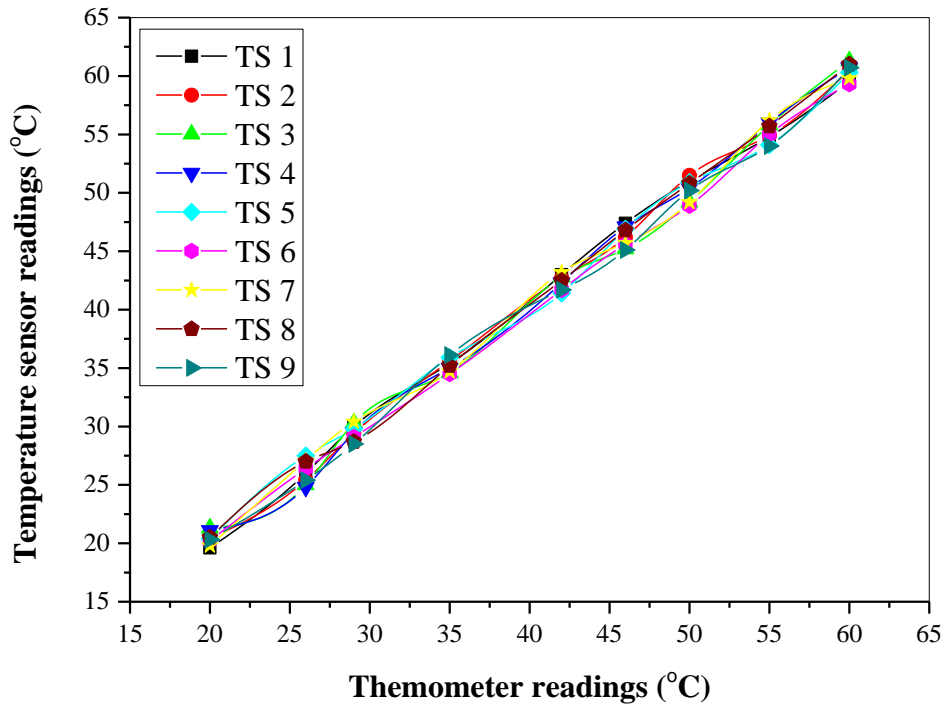


**Figure 3.10:** Temperature sensor calibration graph

### 3.2 Ultra sonicator water bath

Ultra sonicator produces ultrasonic sound wave energy in order to agitate the nanoparticles in base fluid and hence make suspension stable for longer time period. It is shown in the figure 3.11.



**Figure 3.11:** Ultra sonicator water bath

### 3.3 Thermal properties analyzer KD2 PRO

Thermal conductivity of nanofluid was measured by KD2 PRO. It is hand held type instrument with a sensor which is inserted in medium to measure conductivity. Single-needle KS-1 60 mm small sensor as shown in Fig. 3.12 is used to measure the thermal conductivity and resistivity of fluid. The small size of the needle is designed primarily for liquid samples and insulating materials, which have short heating time. A very small amount of heat is applied to the needle which helps to prevent free convection in liquid samples.

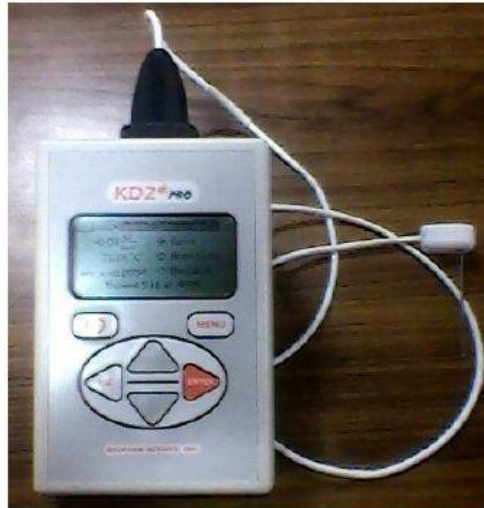


**Figure 3.12:** KD2 Pro with KS-1 needle

**Table 3.3:** Specification single-needle (KS-1)

Size	1.3 mm diameter x 60 mm long
Range	0.02 to 2.00 W/(m· K) (thermal conductivity) 50 to 5000 °C-cm/W (thermal resistivity)
Accuracy (Conductivity)	± 5% from 0.2 - 2 W/(m· K) ±0.01 W/(m· K) from 0.02 - 0.2 W/(m· K)
Cable length	0.8m

### 3.4 Brookfield DV-III Rheometer

Viscosity of nanofluid was measured using Brookfield DV-III Rheometer.. It gives fluid parameter like shear stress and the viscosity at the given shear rate. The principle of operation of the DV-III is that the spindle is driven by means of a calibrated spring, which can measure the viscous drag of the fluid against the spindle by deflection of the spring. A rotary

transducer is present to measure the spring deflection. Rotational speed of the spindle measures the range of a DV-III in centipoises as shown in Fig.3.13 and specification are given in table .



**Figure 3.13:** Brookfield DV-III Rheometer

**Table 3.4:** Specification Brookfield DV-III Programmable Rheometer

Speed Range	0-250 RPM, 0.1 RPM increments
Viscosity Accuracy	±1.0% of full scale range for a specific spindle running at a Specific speed.
Temperature sensing range	- 100°C to 300°C (-148°F to 572°F)
Temperature accuracy	±1.0°C from -100°C to 150°C ±2.0°C from +150°C to 300°C
Analog torque output	0 - 1 Volt DC (0 - 100% torque)
Analog temperature output	0 - 4 Volts DC (10mv / °C)

# Chapter 4

## Methodology and Calculations

---

### 4.1 Preparation of nanofluids

The  $\alpha$ -Al<sub>2</sub>O<sub>3</sub> nanoparticles of average size 40nm were purchased from Intelligent Materials Pvt. Ltd, Panchkula. The properties of Al<sub>2</sub>O<sub>3</sub> nanoparticles are given in table 4.1.

**Table 4.1:** Properties of the Al<sub>2</sub>O<sub>3</sub> nanoparticles [1].

Chemical Name	$\alpha$ -Al <sub>2</sub> O <sub>3</sub> nanopowder
Appearance	White powder
Purity	>99%
Average particle size	40nm
p <sup>H</sup>	6.6
Density (Kg/m <sup>3</sup> )	3970

Nanofluids were prepared by two step method. The nanoparticles were dispersed into the base fluid i.e. water and ethylene glycol mixture in 60:40 ratio. For the required volume concentrations of 0.05%, and 0.1%, fixed quantities of 2.0947 gm and 4.1980 gm of nanoparticles per 1000 ml of base fluid were dispersed respectively. The nanoparticle concentrations were selected because after studying literatures it was observed that up to 0.1% concentrations the nanofluids exhibited very good stability. To further hold the particles in suspension the nanoparticles, ultra sonicator was used. Sonication was done for 2 hours before testing thermal conductivity and viscosity of the nanofluids. After this process the nanoparticles were more evenly dispersed in base fluid. The Al<sub>2</sub>O<sub>3</sub> samples prepared are as shown in Fig. 4.1.



**Figure.4.1:** 0.1% volume concentration Al<sub>2</sub>O<sub>3</sub>/water and ethylene glycol (60:40) nanofluid

## 4.2 Experimental procedure

Experimental setup consisting of a cross flow heat exchanger placed at one end of duct with a force draft fan fixed to other end having varying rpm to change the velocity of air. Duct is 1.25 m in length to produce a uniform flow of air throughout the cross flow heat exchanger. Fluid reservoir having a heater of 3000W with power supply regulated by PID controller was used. Temperature sensors are located on heat exchanger to get the air side temperature readings and four sensors are inserted in heat exchanger to measure the hot fluid temperature at both inlet and outlet. A U-tube mercury manometer was used to determine the fluid side pressure drop.

The above mentioned experimental setup was used for heat transfer rate and pressure drop calculations have been described below.

1. Electrical heater was switched on which is connected to the PID controller to maintain the required inlet temperature. Three temperatures taken were 45°C, 50°C, and 55°C. First we set 45°C temperature for measuring..
2. Pump was used to circulate the hot fluid in heat exchanger circuit as described.
3. Hot fluid consists of base fluid and nanofluid which contain Al<sub>2</sub>O<sub>3</sub> nanoparticle at 0.05% conc. and 0.1% conc. in base fluid.
4. Another pump was used as agitator to maintain the suspension of nanoparticle in base fluid and avoid the local heating of fluid near the heating element to maintain the same temperature throughout the reservoir.
5. First base fluid was used as hot fluid for experimental procedure. Base fluid readings were then compared with nanofluid readings to see the changes.
6. The flow rate of hot fluid flowing in heat exchanger was set. Three different flow rates were taken i.e. 3, 4 and 5 litres per minute respectively.
7. The bypass line valve was set to get minimum flow rate through it and maximum required flow rate through the rotameter.

8. The fan was switched on and velocity set at which the readings were to be taken. There were 3 different velocities settings for fan i.e. 3.30 m/s, 5.30 m/s and 6.4 m/s. For first experimental readings the velocity was set at 3.30 m/s.
9. Temperature readings were noted every 5 min for all the temperature sensors through the digital temperature indicator till steady state was achieved. Pressure drop readings were noted from U tube manometer.
10. Two readings were noted at steady state for all the temperature sensors.
11. The flow rate of hot fluid was changed to 3, 4, and 5 litres per minute and the same steps 9 and 10 were repeated.
12. Then the fan speed was set to 5.30 m/sec after and steps 9 to 11 were repeated.
13. When tests at all three speeds were done then temperature was set at 50°C and the procedure was repeated from step 7.
14. The same procedure from step 7 was repeated again for 55°C temperature and the temperature readings were noted at steady state.
15. The procedure was repeated from step 6 for nanofluid at 0.05% and 0.1% concentrations for all flow rates, all fan speeds, and all temperatures.

### 4.3 Experimental calculations

Experimental calculations were done for both water side and air side at 45°C temperature of hot working fluid. Air side thermo physical properties were considered at bulk mean temperature of air passing across the heat exchanger. Hot fluid thermo physical properties were also considered at bulk mean temperature. A control volume as shown below in Fig.4.2 to calculate the different types of area was considered.

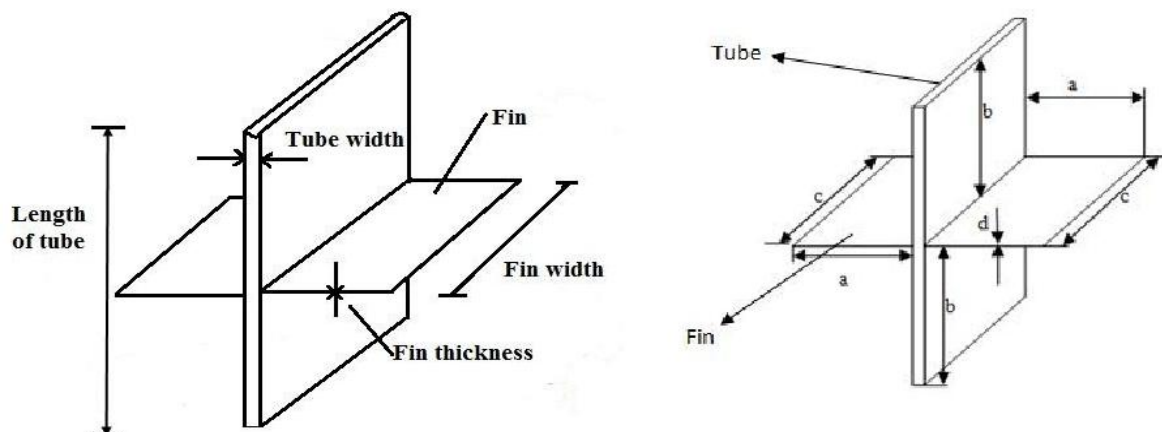


Figure 4.2 Tube fin control volume

#### 4.3.1 Air side calculations

Air side calculation and its thermo physical properties are given below.

$$D_{h,a} = 0.00153 \text{ m} \quad \mu_a = 18.836 \times 10^{-6} \text{ Ns/m}^2 \quad \rho_a = 1.1154 \text{ kg/m}^3 \quad \text{Pr} = 0.71$$

$$K_a = 0.026 \text{ W/mK} \quad C_{p,a} = 1013.3 \text{ J/kg K} \quad V_a = 3.3 \text{ m/s}$$

$$\text{Mass flow rate of air, } W_a = \rho_a \times A_c \times V_a \quad (4.1)$$

$$W_a = 0.11042 \text{ kg/s}$$

$$\text{Heat capacity rate} = W_a \times C_{p,a} \quad (4.2)$$

$$\text{Heat capacity rate} = 111.89 \text{ W/K}$$

$$\text{Core mass velocity [2], } G_a = W_a/A_c \quad (4.3)$$

$$G_a = 3.68 \text{ kg/m}^2\text{s}$$

$$\text{Re}_a = G_a \times D_{h,a} \div \mu_a = 299 \quad (4.4)$$

$$\text{Reynolds number louvered side, } \text{Re}_{lp} = \rho_a \times l_p \times V_a / \mu_a \quad (4.5)$$

$$\text{Re}_{lp} = 164.2$$

Colburn factor ( $J_a$ ) is dimensionless representation of heat transfer coefficient [2]

$$J_a = 0.249 \times \text{Re}_{lp}^{-0.42} \times l_h^{0.33} \times H^{0.26} \times l_l^{1.1}/H_f \quad (4.6)$$

$$J_a = 0.010$$

$$h_a = J_a \times G_a \times C_{p,a}/\text{Pr}_a^{2/3} \quad (4.7)$$

$$h_a = 46.854$$

$$m = (2 \times h_a/K_a \times \delta)^{0.5} = 0.36 \quad (4.8)$$

$$ml = 0.36 \times 3.5/1000 = 0.00126$$

$$\text{Fin efficiency } \eta_f = \tanh ml / ml \quad (4.9)$$

$$\eta_f = 0.98$$

### 4.3.2 Hot working fluid tube side

Hot fluid side calculation and thermo physical properties for the base fluid are given below at 3 litres per minute flow rate

$$D_{h,bf} = 0.0013623 \text{ m} \quad \mu_{bf} = 0.001546 \text{ Ns/m}^2 \quad \rho_{bf} = 1092 \text{ kg/m}^3 \quad \text{Pr}_{bf} = 8.66$$

$$K_{bf} = 0.424 \text{ W/mK} \quad C_{p,bf} = 3560 \text{ J/kg K} \quad V_{bf} = 0.094 \text{ m/s}$$

$$\text{Mass flow rate of base fluid, } W_{bf} = 0.0546 \text{ kg/s}$$

$$\text{Heat capacity rate} = W_{bf} \times C_{p,bf} \quad (4.10)$$

$$\text{Heat capacity rate} = 194.376$$

$$\text{Reynold number through each tube, } \text{Re}_{bf} = \rho_{bf} \times V_{bf} \times D_{h,bf} / \mu_{bf}$$

$$\text{Re}_{bf} = 90.23$$

$$h_{bf} = K_{bf} \times \text{Nu}_{bf} / D_{h,bf}$$

$$h_{bf} = 1436.460 \text{ W/m}^2\text{K}$$

## References

- [1]. Intelligent material Pvt. Ltd. [www.nanoshel.com](http://www.nanoshel.com).
- [2]. Gangacharyulu D, Sharma J.K., Singh G, “Performance evaluation of after cooler in diesel engines- A case study” , IE(I) journal-MC, Vol 80, May 1999.
- [3]. <http://www.mhtl.uwaterloo.ca/old/onlinetools/airprop/airprop.html>

# Chapter 5

## Results and Discussion

### 5.1 Temperature dependence of thermo-physical properties

Various thermo physical properties of the nanofluid namely the thermal conductivity, density and viscosity were measured experimentally with the help of KD2 Pro thermal property analyzer, specific gravity bottle and Brookfield DV-III Rheometer respectively. Temperature dependence of these properties was also studied experimentally which were then compared with those of the base fluid.

#### 5.1.1 Temperature dependence of density of nanofluid

From Figure 5.1, it could be concluded that nanofluid density was higher than that of water as was expected but it decreased slightly with increase in temperature of the fluid. There was a maximum variation of only 1.01% when temperature increased from 25 °C to 65 °C .

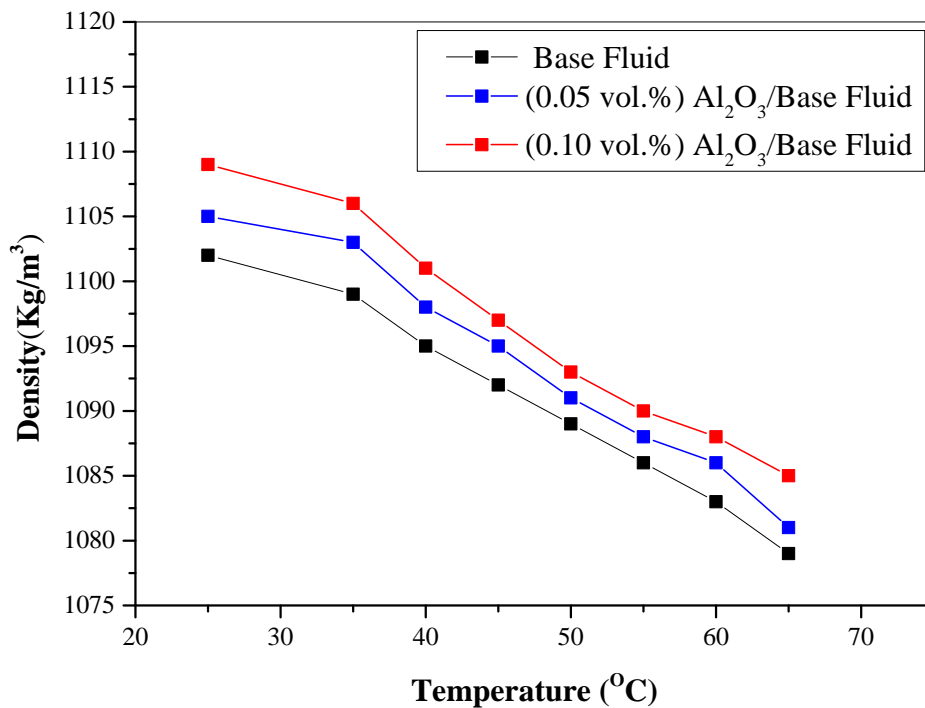


**Figure 5.1:** Effect of temperature variation on density of Al<sub>2</sub>O<sub>3</sub>/water and ethylene glycol nanofluid.

The trend of change in density was similar to the trend shown by the base fluid which was mixture of water and ethylene glycol in 60:40 ratio.

### 5.1.2 Temperature dependence of thermal conductivity of nanofluid

From experimental data it was observed that the thermal conductivity of  $\text{Al}_2\text{O}_3$ /water and ethylene glycol nanofluid was higher than that of water and ethylene glycol which was the base fluid. Also it showed strong dependency on temperature of the fluid. Figure 5.2 shows the experimental data of thermal conductivity of nanofluid which increased significantly with the base fluid temperature. The reason can be attributed to the fact that increase in fluid temperature further strengthens the Brownian motion of dispersed nanoparticles and also reduces the viscosity of the base fluid. Along with a strengthened Brownian motion of particles, the effect of micro convection in heat transport increases and as a result it increased the thermal conductivity of nanofluids.

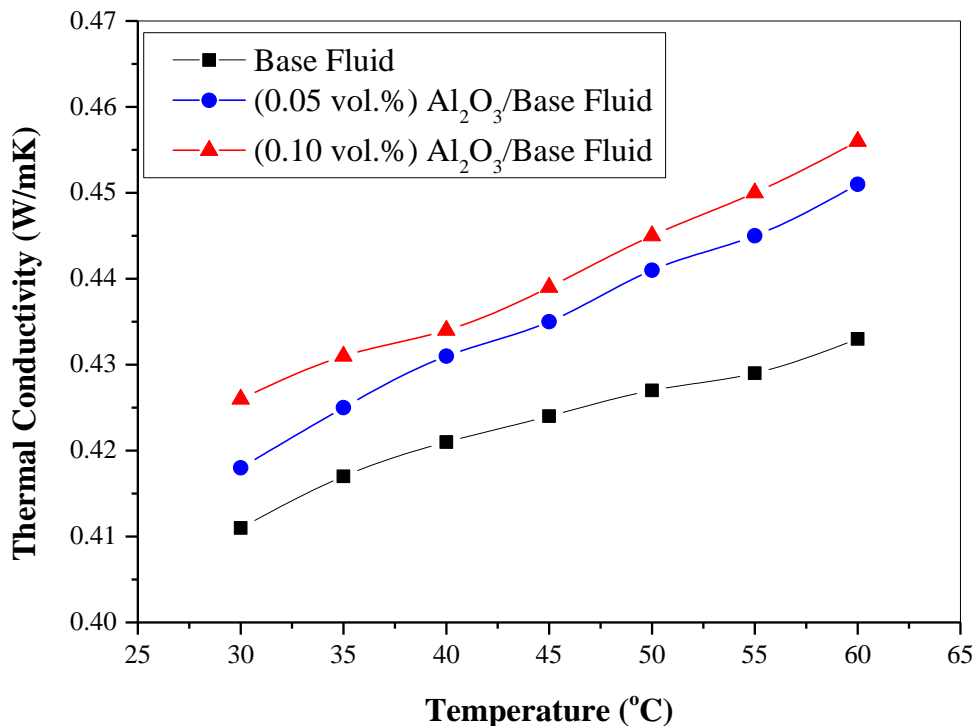


**Figure 5.2:** Dependence of Thermal Conductivity of  $\text{Al}_2\text{O}_3$ /water and ethylene glycol nanofluid with temperature.

### 5.1.3 Temperature dependence of viscosity of nanofluid

From the experimental data obtained, it was observed that viscosity of nanofluid at 0.1% (vol.) concentration was slightly higher than that of water, simply because when solid particles are added to the base fluid, it increased the density of the mixture and as a result it

required more force to overcome the inertial forces. Hence the viscosity increased but there was significant variation in viscosity with changes in temperature. The trend of change in viscosity was similar to the trend shown by the base fluid as shown by the figure 5.3 below.

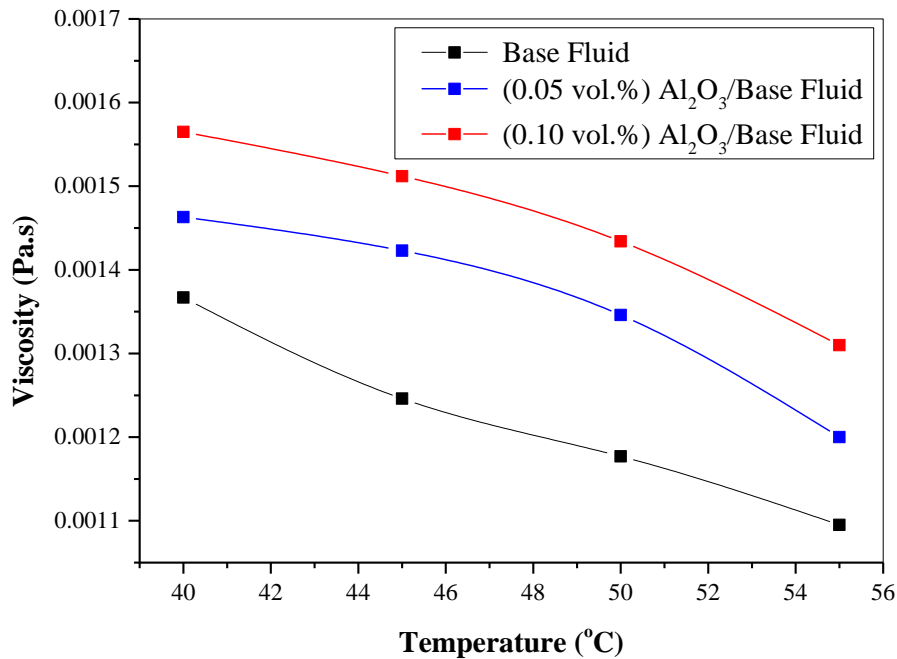


**Figure 5.3:** Effects of temperature on viscosity of nanofluid.

## 5.2 Tube side analysis of working fluid

Experiments were performed at varying temperatures and inlet flow rates of working fluid, using base fluid and two different concentrations of Al<sub>2</sub>O<sub>3</sub> nanoparticles. Heat transfer rate was increased significantly with addition of nanoparticles into base fluid primarily due to the increased thermal conductivity of base fluid. To understand the changes in heat transfer coefficient, the changes in Nusselt number were observed because Nusselt number is a dimensionless form of heat transfer co-efficient.

Friction factor, which is a measure of pressure drop, was also another important parameter that was observed. The thermal performance of the heat exchanger was improved significantly along with slight increase in the pumping power after the addition of nanoparticles. The tube side performance characteristics were observed by analyzing the following parameters. The effect on Reynolds number of working fluid, inlet temperature and nanoparticles concentration on tube side Nusselt number and friction factor have been illustrated as follows.

### 5.2.1 Temperature dependence of Reynolds number at different flow rates

Reynolds number is a measure of flow pattern. For laminar flow through pipes and tubes its value is below 2000. Figure 5.4 shows the effect on Reynolds number for base fluid and particle volume concentrations of 0.05% and 0.1 % at different inlet temperatures of 45°C, 50°C, 55°C along with different flow rates of 3, 4, 5 Litre per minute (LPM). Similar trends were found for higher values of temperature. The enhancement of heat transfer with rising Reynolds number was observed primarily due to reduction of the thermal boundary layer thickness.

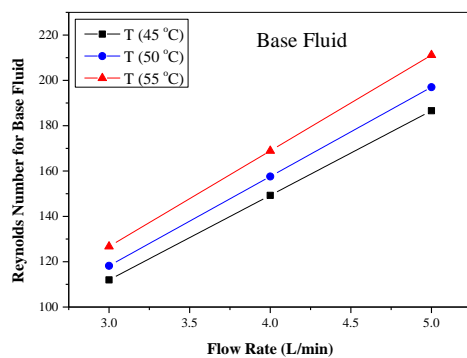


Figure 5.4(a): Reynolds number for base fluid

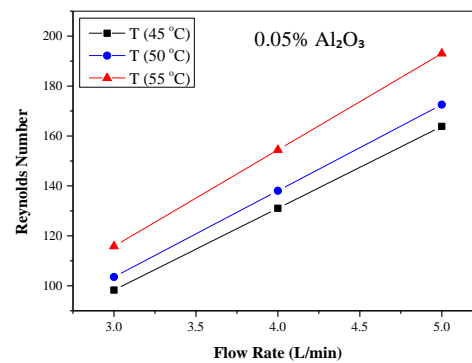


Figure 5.4(b): Reynolds number for 0.05% Al<sub>2</sub>O<sub>3</sub>

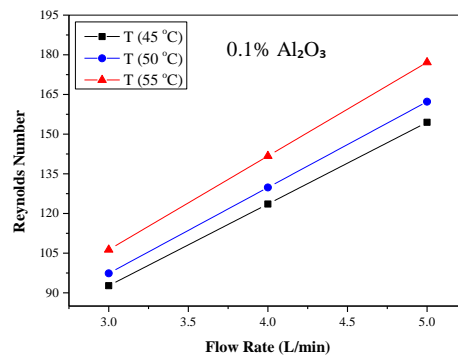


Figure 5.4(c): Reynolds number for 0.1% Al<sub>2</sub>O<sub>3</sub>

From the data it was observed that although the trends were similar but the actual values of Reynolds number were different due to different fluid properties of the base fluids at different temperatures namely the viscosity and density.

### 5.2.2 Temperature dependence of Nusselt number at different flow rates

Nusselt number is a dimensionless measure of heat transfer coefficient. Figure 5.5 shows the effect on Nusselt number for base fluid and particle volume concentrations of 0.05% and 0.1 % at different inlet temperatures of 45°C, 50°C, 55°C along with different flow rates of 3, 4,

5 Litre per minute (LPM). Similar trends were found for higher values of temperature. The enhancement of heat transfer with rising Nusselt number was observed.

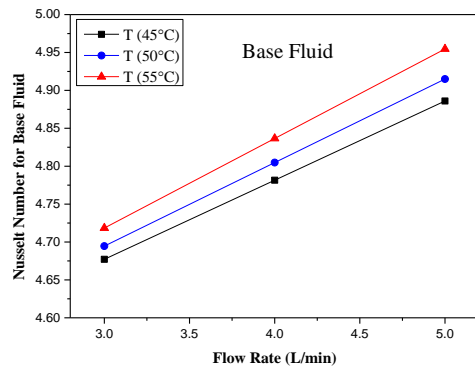


Figure 5.5(a): Nusselt number for base fluid

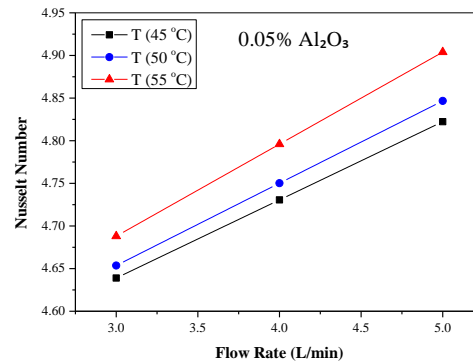


Figure 5.5(b): Nusselt number for 0.05% Al<sub>2</sub>O<sub>3</sub>

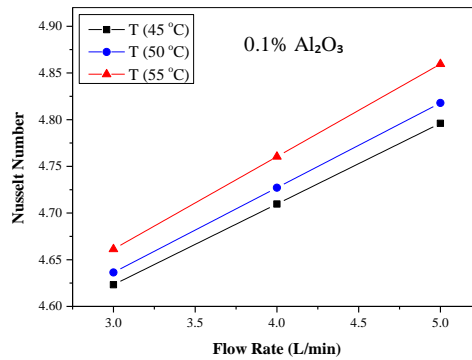


Figure 5.5(c): Nusselt number for 0.1% Al<sub>2</sub>O<sub>3</sub>

It can be clearly seen from the data the variation trends were similar to the one shown by the base fluid. It can also be interpreted that Nusselt numbers significantly increased with increasing Reynolds number which itself increased with increasing flow rates as showed in figures 5.4.

### 5.2.3 Temperature dependence of friction factor at different flow rates

Friction factor is the measure of pressure drop and therefore signifies the pumping power required to pump the working fluid through the heat exchanger. As shown in figure 5.6 friction factor of base fluid decreased as the Reynolds number increased at the given temperature but it was also observed that as the temperature was increased the value of friction factor decreased because in the case of liquids the Reynolds number increases due to decrease in viscosity. Friction factor was observed to decrease considerably with increasing flow rates, simply because at higher flow rates the Reynolds number also increased because the inertial forces become dominant as compared to the viscous forces. At this stage the

addition of nanoparticles increased the friction factor which showed that the use of nanofluids for heat transfer enhancement did increase the required pumping power.

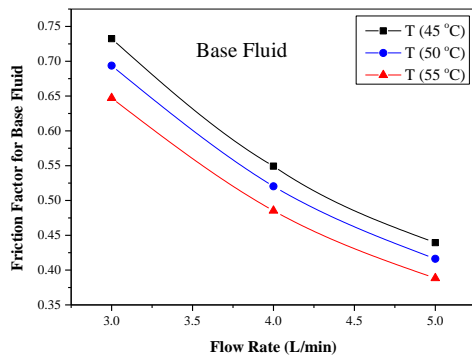


Figure 5.6(a): Friction factor for base fluid

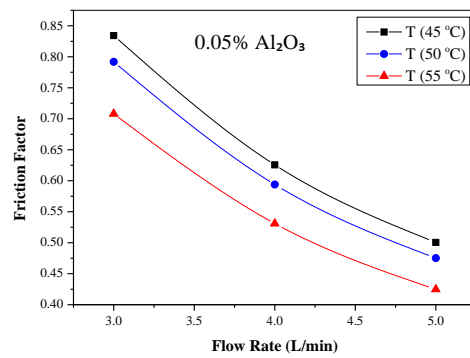


Figure 5.6(b): Friction factor for 0.05% Al<sub>2</sub>O<sub>3</sub>

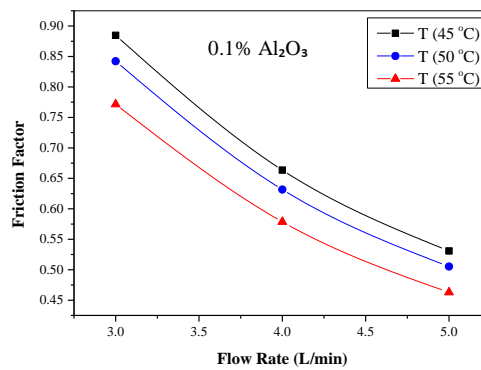
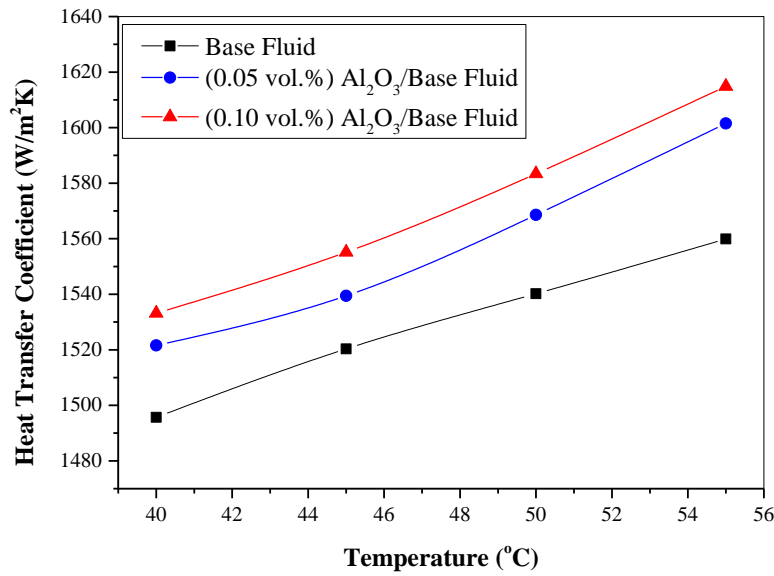


Figure 5.6(c): Friction factor for 0.1% Al<sub>2</sub>O<sub>3</sub>

## 5.2.4 Heat transfer coefficient variation with nanofluid concentration

The tube side heat transfer coefficient increased as the nanoparticle concentration was increased as shown in figure 5.7. It was also observed that with increasing inlet temperature of the fluid the heat transfer coefficient increased with a maximum enhancement of 3.54% for 0.1% vol. concentration and a minimum enhancement of 1.87% for 0.05% vol. concentration of Al<sub>2</sub>O<sub>3</sub> nanoparticles. The minimum enhancement was observed at 40 °C temperature and maximum enhancement was observed at 55 °C temperature. From the graph it was also observed that for 0.1% vol. concentration the increase in enhancement was relatively small over 0.05% vol. concentration as compared to the base fluid.



**Figure 5.7:** Effects of temperature on heat transfer coefficient at different concentrations.

### 5.2.5 Variation in pressure drop

The experiment was conducted with a U tube manometer connected across the inlet and outlet of the heat exchanger to measure the direct pressure drop through it. The data is plotted in figure 5.8 as shown below. It was observed that the pressure drop increased with the increasing concentration of nanoparticles as was expected. The maximum increase in pressure drop was observed to be 20% for 0.1% vol. concentration of Al<sub>2</sub>O<sub>3</sub> nanoparticles. Whereas for 0.05% vol. concentration the maximum pressure drop was observed to be around 12%.

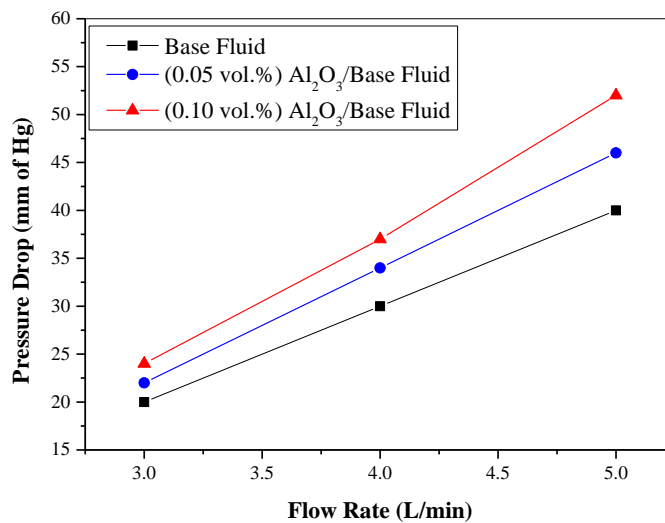


**Figure 5.8:** Tube side pressure drop at different concentrations.

# Chapter 6

## Conclusions

---

The experiments were conducted on a single-pass multiple tube cross-flow heat exchanger to study the effect of  $\text{Al}_2\text{O}_3$ /water and ethylene glycol nanofluid on the thermo hydraulic performance characteristics of the heat exchanger. The experiments were conducted using mixture of water and ethylene glycol in 60:40 ratio as base fluid, 0.05% (vol.) and 0.1% (vol.) concentration  $\text{Al}_2\text{O}_3$ /water and ethylene glycol nanofluid as hot working fluid flowing through the heat exchanger tubes.

The experiments were conducted at 45°C, 50°C and 55°C fluid temperature at inlet. Reynolds number of working fluid and air flowing across the heat exchanger was varied at three different settings. The tests were carried out in laminar flow regime and the following conclusions were made based on the data from the experiment performed.

### 6.1 Thermo physical Properties

- Thermal conductivity of base fluid was increased with the addition of nanoparticles. Also it was observed that thermal conductivity showed dependence on temperature. Enhancement of 6.58 % in thermal conductivity was seen at 30 °C while it was 8.23 % at 60°C.
- Density of nanofluid was observed to be slightly higher than the base fluid. But with increasing the temperature its density decreased. Density showed a variation of 1.01% as temperature increased from 25°C to 65°C.
- Viscosity of nanofluid was also higher than that of base fluid as was expected, and it followed a decreasing trend with increase in temperature. Viscosity of nanofluid showed a variation of 9.57% as temperature increased from 40°C to 55°C with a maximum increase of 19.1% over the base fluid for 0.1% vol. concentration sample.

### 6.2 Heat exchanger tube side performance

- Nusselt number of hot working fluid was increased with increasing flow rate of fluid and nanoparticles volume concentration. For 45°C inlet fluid temperature, Nusselt

number was increased by 3.9% and 4.5% for 0.05% and 0.1% vol. concentration of nanofluids, respectively.

- Nusselt number also showed an increase with increasing the inlet temperature of hot working fluid. For 0.05% particle volume concentration, value of Nusselt number was increased by 5.38% and 5.85% for 0.05% and 0.1% vol. concentrations respectively when temperature was increased to 55°C from 45°C.
- The heat transfer coefficient increased with a maximum enhancement of 3.54% for 0.1% vol. concentration and a minimum enhancement of 1.87% for 0.05% vol. concentration of Al<sub>2</sub>O<sub>3</sub> nanoparticles.
- Friction factor of hot working fluid showed an increase with addition of nanoparticles into the base fluid. At 45°C inlet temperature of nanofluid the friction factor increased by 13.9% and 20.81% for 0.05% and 0.1% nanoparticle volume concentrations respectively over the base fluid.
- The average friction factor of nanofluid decrease with increasing inlet temperature of nanofluid. For 0.05% vol. concentration, friction factor was decreased by 14.28% and for 0.1% vol. concentration it decreased by 12.6% when temperature was increased to 55°C from 45°C.

### **6.3 Heat exchanger overall performance**

- The effectiveness of the heat exchanger was increased with the aid of Al<sub>2</sub>O<sub>3</sub>/Water and ethylene glycol (60:40) nanofluids. It increased by 11.19 % and 18.72% for 0.05% and 0.1% vol. concentrations of nanofluids respectively.
- The overall heat transfer co-efficient based on the fin side heat transfer area was also increased by 7.21% and 12.64% for 0.05% and 0.1% vol. concentrations respectively as compared to the base fluid.

### **6.4 Future scope**

The presented work was done utilizing Al<sub>2</sub>O<sub>3</sub>/water and ethylene glycol (60:40) nanofluid which was prepared by two step method. Al<sub>2</sub>O<sub>3</sub> nanoparticles of average particle size 40 nm were dispersed into the base fluid at 0.05% and 0.1% volume concentrations. Future scopes of the work are as follows.

- Experiments can be performed using smaller sized particles, less than 40 nm, as it would help in stabilizing the nanofluid and avoid settling down of particles.
- CFD analysis needs to be done extensively to get results comparable to the experimental results.
- Better understanding required for two phase CFD analysis because single phase analysis gives comparable results only for very low particle concentrations.

# Appendix

**Table A1:** Rotameter calibration data

Flow rate (LPM)	Flow rate (ml per 30 second)	Test 1	Test 2	Test 3	Test 4	Test 5	Test 6	Test 7	Test 8	Test 9	Test 10
2	1000	1010	1004	998	990	992	1006	990	996	1003	1007
3	1500	1515	1506	1497	1485	1488	1509	1485	1494	1504	1510
4	2000	2020	2008	1996	1980	1984	2012	1980	1992	2006	2014
5	2500	2520	2510	2495	2490	2485	2510	2490	2488	2507	2515
6	3000	3010	3012	2994	2985	2990	3015	2985	2988	3009	3015

**Table A2:** Temperature sensors calibration data (°C)

Thermometer reading	TS 1	TS 2	TS 3	TS 4	TS 5	TS 6	TS 7	TS 8	TS 9
20	19.6	20.4	21.3	21.1	20.4	20.2	19.8	20.5	20.3
26	26	25.4	25	24.8	27.5	26.4	27.1	27	25.4
29	30	29.4	30.3	29.5	29.8	29.1	30.4	28.7	28.5
35	35.4	35.6	34.6	35	35.9	34.5	34.7	35.2	36.1
42	43	42.7	42.8	42.3	41.4	41.7	43.2	42.5	41.7
46	47.4	46.2	45.2	47.1	46.9	45.6	45.7	46.8	45.1
50	51	51.5	49.2	50.4	50.9	48.9	49.2	50.8	50.2
55	54.8	54.9	55.8	56	54.1	55	56.2	55.7	54
60	59.5	60.5	61.3	60.7	60.3	59.3	59.8	61	60.7

**Table A3:** Thermal Conductivity of Al<sub>2</sub>O<sub>3</sub>/water and ethylene glycol nanofluid with temperature.

Temperature (°C)	Thermal conductivity (W/mK)		
	Base fluid	0.05%	0.10%
30	0.411	0.418	0.426
35	0.417	0.425	0.431
40	0.421	0.431	0.434
45	0.424	0.435	0.439
50	0.427	0.441	0.445
55	0.429	0.445	0.45
60	0.433	0.451	0.456

**Table A4:** Viscosity of nanofluid with temperature

Temperature (°C)	Viscosity (Pa. s) <sup>2</sup>		
	Base fluid	0.05%	0.10%
40	0.001367	0.001463	0.001565
45	0.001246	0.001423	0.001512
50	0.001177	0.001346	0.001434
55	0.001095	0.0012	0.00131

**Table A5:** Reynolds number with temperature.

Flow Rate (LPM)	Reynolds number for Base Fluid			Reynolds number for 0.05 % conc.			Reynolds number for 0.1 % conc.		
	45°C	50°C	55°C	45°C	50°C	55°C	45°C	50°C	55°C
3	111.95762	118.1954	126.6965	98.30108	103.5449	115.8235	92.68382	97.36886	106.2929
4	149.27683	157.5938	168.9287	131.0681	138.0599	154.4313	123.5784	129.8251	141.7239
5	186.59604	196.9923	211.1609	163.8351	172.5749	193.0392	154.473	162.2814	177.1548

**Table A6:** Nusselt number with temperature.

Flow Rate (LPM)	Nusselt number for Base Fluid			Nusselt number for 0.05 % conc.			Nusselt number for 0.1 % conc.		
	45°C	50°C	55°C	45°C	50°C	55°C	45°C	50°C	55°C
3	4.6771631	4.638964	4.623251	4.638964	4.653631	4.687977	4.623251	4.636356	4.661318
4	4.7815508	4.730618	4.709668	4.730618	4.750175	4.795969	4.709668	4.727141	4.760424
5	4.8859385	4.822273	4.796085	4.822273	4.846719	4.903961	4.796085	4.817927	4.85953

**Table A7:** Friction factor with temperature.

Flow Rate (LPM)	Friction factor for Base Fluid			Friction factor for 0.05 % conc.			Friction factor for 0.1 % conc.		
	45°C	50°C	55°C	45°C	50°C	55°C	45°C	50°C	55°C
3	0.73242	0.693767	0.647216	0.834172	0.791927	0.707974	0.884728	0.842158	0.771453
4	0.549315	0.520325	0.485412	0.625629	0.593945	0.53098	0.663546	0.631619	0.57859
5	0.439452	0.41626	0.388329	0.500503	0.475156	0.424784	0.530837	0.505295	0.462872

**Table A8:** Properties of air at 1 atm pressure

Temperature (°C)	Density (kg/m <sup>3</sup> )	Specific heat (J/kg.K)	Thermal conductivity (W/m.K)	Dynamic Viscosity (Pa.s)	Prandtl number (Pr)
20	1.204	1007	0.02514	1.825	0.7309
25	1.184	1007	0.02551	1.849	0.7296
30	1.164	1007	0.02588	1.872	0.7282
35	1.145	1007	0.02625	1.895	0.7268
40	1.127	1007	0.02662	1.918	0.7255
45	1.109	1007	0.02699	1.941	0.7241
50	1.092	1007	0.02735	1.963	0.7228
60	1.059	1007	0.02808	2.008	0.7202

**Table A9:** Temperature data for 45°C fluid temperature at 3 LPM flow rate and air velocity of 3.3 m/s

No.	T1	T2	T3	T4	T5	T6	T7	T8	T9
1	26	49.1	20.2	45.3	43	42.6	50.5	37.7	38.4
2	25.8	49.2	20.1	44.9	42.8	42.4	50.7	37.6	38.2
3	25.7	48.9	20.1	44.9	42.7	42.5	50.7	37.5	38
4	25.4	48.8	20	44.9	42.6	42.6	50.8	37.2	37.8
5	25.4	49.3	20	44.9	42.7	42.6	50.7	37.3	37.9
6	25.4	48.8	20	44.9	42.7	42.6	50.7	37.3	37.7
7	25.4	48.8	20	44.9	42.7	42.6	50.7	37.3	37.7